Meteoritics & Planetary Science 41, Nr 5, 749–771 (2006)
Abstract available online at http://meteoritics.org

The record of Miocene impacts in the Argentine Pampas

Peter H. SCHULTZ[1*], Marcelo ZÁRATE[2], Willis E. HAMES[3], R. Scott HARRIS[1], T. E. BUNCH[4], Christian KOEBERL[5], Paul RENNE[6], and James WITTKE[7]

[1]Department of Geological Sciences, Brown University, Providence, Rhode Island 02912–1846, USA
[2]Facultad de Ciencias Exactas y Naturales, Universidad Nacional de La Pampa, Avda Uruguay 151, 6300 Santa Rosa, La Pampa, Argentina
[3]Department of Geology, Auburn University, Auburn, Alabama 36849, USA
[4]Department of Geology, Northern Arizona University, Flagstaff, Arizona 86011, USA
[5]Department of Geological Sciences, University of Vienna, Althanstrasse 14, A-1090 Vienna, Austria
[6]Berkeley Geochronology Center, 2455 Ridge Road, Berkeley, California 94709, USA
[7]Department of Geology, Northern Arizona University, Flagstaff, Arizona 86011, USA
[*]Corresponding author. E-mail: peter_schultz@brown.edu

(Received 02 March 2005; revision accepted 14 December 2005)

Abstract–Argentine Pampean sediments represent a nearly continuous record of deposition since the late Miocene (~10 Ma). Previous studies described five localized concentrations of vesicular impact glasses from the Holocene to late Pliocene. Two more occurrences from the late Miocene are reported here: one near Chasicó (CH) with an $^{40}Ar/^{39}Ar$ age of 9.24 ± 0.09 Ma, and the other near Bahía Blanca (BB) with an age of 5.28 ± 0.04 Ma. In contrast with andesitic and dacitic impact glasses from other localities in the Pampas, the CH and BB glasses are more mafic. They also exhibit higher degrees of melting with relatively few xenoycrysts but extensive quench crystals. In addition to evidence for extreme heating (>1700 °C), shock features are observed (e.g., planar deformation features [PDFs] and diaplectic quartz and feldspar) in impact glasses from both deposits. Geochemical analyses reveal unusually high levels of Ba (~7700 ppm) in some samples, which is consistent with an interpretation that these impacts excavated marine sequences known to be at depth. These two new impact glass occurrences raise to seven the number of late Cenozoic impacts for which there is evidence preserved in the Pampean sediments. This seemingly high number of significant impacts over a 10^6 km^2 area in a time span of 10 Myr is consistent with the number of bolides larger than 100 m expected to enter the atmosphere but is contrary to calculated survival rates following atmospheric disruption. The Pampean record suggests, therefore, that either atmospheric entry models need to be reconsidered or that the Earth has received an enhanced flux of impactors during portions of the late Cenozoic. Evidence for the resulting collisions may be best preserved and revealed in rare dissected regions of continuous, low-energy deposition such as the Pampas. Additionally, the rare earth element (REE) concentrations of the target sediments and impact melts associated with the Chasicó event resemble the HNa/K australites of similar age. This suggests the possibility that those enigmatic tektites could have originated as high-angle, distal ejecta from an impact in Argentina, thereby accounting for their rarity and notable chemical and physical differences from other Australasian impact glasses.

INTRODUCTION

Vast deposits of upper Tertiary to Holocene loess and loess-like (loessoid) sediments cover the Argentine Pampas. These deposits began to develop during the late Miocene in response to the Andean orogeny and ensuing climatic changes (Zárate 2003). The late Quaternary loess record has received increasing attention for interpreting the continental paleoclimates in this part of the southern hemisphere (Muhs and Zárate 2001; Zinck and Sayago 1999; Orgeira et al. 1998; Iriondo 1997). The early history, however, is less extensively researched due to the limited chronostratigraphic markers and the very limited paleomagnetic studies.

Enigmatic glasses within these sediments are locally called “escorias” and often are associated with (and attached to) reddish, brick-like masses called “tierra cocidas.” The term “escoria” can imply a wide range of vesicular glasses (e.g., volcanic or human-produced slag). Because they occur

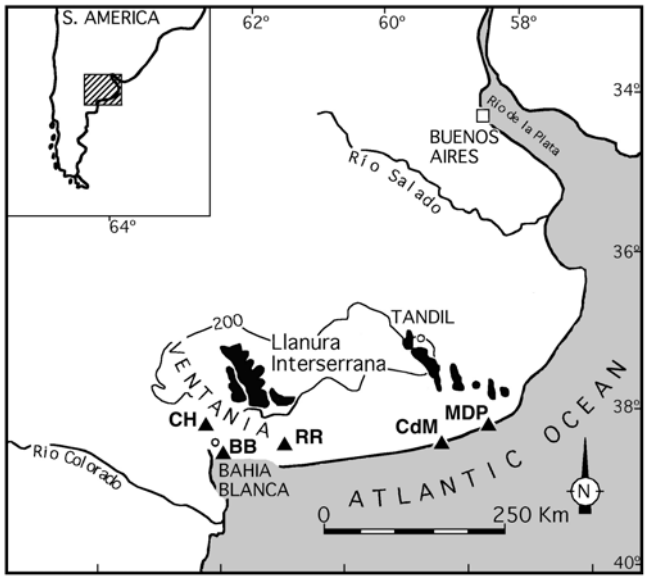

Fig. 1. A map showing the primary locations where Chasicó (CH) and Bahía Blanca (BB) glasses have been investigated. Related glasses occur in Mio/Pliocene outcrops along a railroad cut (RR) near BB and at other sites scattered throughout southern Buenos Aires Province. Pliocene and Pleistocene impact glasses occur in the vicinities of Mar del Plata (MDP) and Centinela del Mar (CdM), respectively.

in large quantities at specific horizons within pre-Holocene sediments, a different origin is required, especially in the absence of nearby volcanic sources. Studies of such glasses in Late Pliocene to Holocene Pampean sediments have established that they were formed as the result of hypervelocity impact (Schultz et al. 1994; 1998; 2004; Harris et al. 2005a, 2005b).

The identification and characterization of older Pampean glasses would not only improve our understanding of possible impact products in the sedimentary record, but also would provide needed chronostratigraphic markers. These older successions contain important fossil assemblages that were proposed to track mammalian evolution and interchanges through time (Pascual et al. 1996; Marshall et al. 1983). Therefore, radiometric dates of instantaneously formed impact glasses provide unique benchmarks for re-evaluating faunal evolution.

Here we report the discovery of two new glass deposits concentrated along specific horizons in late Miocene strata and provide evidence for their impact origin. The oldest glass layer dates to about 9.2 Ma and provides a critical benchmark for important Miocene outcrops. The second concentration dates to about 5.3 Ma, which is approximately the Miocene/Pliocene boundary (Berggren et al. 1995). We first review the Pliocene to Pleistocene impact record in the Pampas of Argentina and then focus on the specific geologic setting of the two new localities. Next, we discuss the nature (including evidence for impact origin) and age of the impact glasses. Lastly, we consider the possible implications, including the size of the events, comparison with other impact glasses in younger sediments, the production rate of glass-producing impacts, and the possible relation to the enigmatic Australian HNa/K tektites with an age similar to that of the Chasicó glasses.

BACKGROUND

Argentine Impact Glasses

At least four impact glass deposits have been discovered in post-Miocene Pampean sediments (Schultz et al. 1994; 1998, 2002a, 2002b, 2004; Bland et al. 2002). These impact glasses often are attached to or wrap around tierra cocidas that are composed of oxidized and welded sediments that are believed to be lower-temperature impact products, the equivalent of clastic breccias derived from unconsolidated sediments (Schultz et al. 1998, 2004). The glasses contain clear evidence for intense, transient heating to temperatures exceeding 1700 °C followed by rapid cooling and dynamic emplacement (Schultz et al. 1994, 1998; Harris et al. 2005a). Shock indicators have been documented in the Pliocene and oldest Pleistocene glasses (Harris et al. 2005a, 2005b).

The two new glass occurrences described in this paper are exposed in sediments of the Southern Buenos Aires (SBA) Province (Fig. 1). The older glasses occur in well-known upper Miocene loessoid strata composed primarily of silty sands containing carbonate nodules and, at certain levels, carbonate cements. These generally unconsolidated deposits contain late Miocene fossil mammal assemblages characterized as the “Chasicóan assemblages” by Fidalgo et al. (1978) and Bondesio et al. (1980). While other materials of Chasicóan age crop out far to the northwest (the central part of La Pampa Province, San Luis, San Juan, and Catamarca), the exposures closer to the Atlantic coast are limited to a very restricted area surrounding Laguna de Chasicó and Salinas Chicas. The Chasicó (CH) glasses in this region are typically 1–10 cm in diameter, but have been found in tightly clustered assemblages as large as 2 m across. Although they do not form a continuous bed of melt, they occur scattered within specific stratigraphic horizons that can be traced for more than 5 km (discussed below).

The second glass layer is widespread in upper Miocene to lower Pliocene outcrops throughout the Southern Buenos Aires (SBA) Province from Bahía Blanca (BB) east into the Arroyo Claromecó Basin (east of the Sierra La Ventana mountain range comprised of Paleozoic basement rocks), and west to near Guaminí. Multiple localities near Bahía Blanca yield the largest concentrations of glasses (up to 10 cm across). Our initial suspicion was that these glasses represented distal equivalents of the Chasicó glasses initially emplaced on the Sierra La Ventana piedmont but transported and reworked into much younger sediments through fluvial

reworking (Schultz et al. 2000). As described below, however, radiometric dates now clearly establish that the BB glasses represent a completely separate event, generally consistent with their present stratigraphic position.

In the following discussion, the Chasicó materials will be described in greater detail because the stratigraphic setting is presently better constrained by field studies, paleomagnetic profiles, and more continuous exposures.

GEOLOGIC SETTING

The Chasicó exposures represent the oldest outcroppings of Miocene sediments in the southern Buenos Aires province (see review by Zárate [2003]). The sediments were deposited in response to enhanced transport processes created by uplift of the Cordilleras during the late Miocene. Zárate et al. (Forthcoming) provide greater details on the lithofacies and detailed stratigraphy of the Arroyo Chasicó Formation.

Along the Chasicó arroyo, silty sands accumulated during the Miocene within a major region of subsidence of the Colorado Basin. Sediments were derived from the nearby piedmont of the Sierra La Ventana range combined with fluvial and aeolian transport from the Andes far to the west. Based on geophysical surveys, the sediments extend to a total depth of 5 km, with deposits similar to the exposed Chasicóan-age (defined by the contained faunal assemblages) materials extending down 180 m (Zambrano 1980; Bonorino et al. 1987). The Chasicó Arroyo cuts through and exposes the upper portion of these upper Miocene deposits as it discharges into Laguna Chasicó. Tertiary marine sequences occur below the Chasicóan sediments nearby.

North and east of Laguna de Chasicó, upper Tertiary deposits form an extensive and gentle plain descending from nearly 400 m in the Sierra de la Ventana to elevations of about 50 m in Bahía Blanca on the Atlantic coast and around 70–80 m at the northern margin of the Chasicó depression. A 1.5–2 m thick calcrete crust caps the deposits, which are overlain by the upper Pleistocene-Holocene sandy aeolian mantle. The present drainage system carves into these upper Tertiary sequences, which crop out discontinuously along riverbanks, road cuts, and in quarries. North and west of Sierra de la Ventana, the upper Tertiary deposits form a vast plain extending into La Pampa Province, where they are grouped into the Cerro Azul Formation.

Folded and twisted glassy masses (along with tierra cocidas) outcrop along a 5 km section near the lower reaches of the Arroyo Chasicó. Zárate et al. (Forthcoming) provide a more detailed discussion of the revised stratigraphy of these sequences. There are three occurrences: 1) a concentration of large masses just above a paleosol within sandy fluvial facies, 2) larger angular glass fragments within a lower diamicton (CH-LM), and 3) dispersed smaller and broken fragments in a series of upper diamicton layers (CH-U). This pattern is very similar to occurrences near Chapadmalal (Schultz et al. 1998, 2002a, 2002b) and is interpreted as a lower, primary glass-bearing layer that was subsequently covered by rapidly reworked sediments from nearby exposures of the lower primary unit. Although it is possible that the diamicton deposit could represent primary ejecta facies, such an interpretation cannot yet be tested.

Glasses were also recovered from upper Tertiary deposits that crop out in the surroundings of Bahía Blanca, as well as further east in various isolated upper Miocene outcrops including railroad cuts (labeled “RR”) and exposures along the Arroyo Claromecó valley at distances of about 250 km from Bahía Blanca. Near Bahía Blanca, the glasses occur in fluvial/aeolian sequences that are part of a vast structural plain descending from the Ventana Range to the Atlantic Ocean. One particular section is about 20 m thick. The lowermost 5 m are composed of massive light brown siltstones, which contain partially silicified calcareous nodules up to 70 cm long. The upper 15 m of the exposure is made up of light brown calcareous siltstones, either massive or displaying coarse stratification that suggests aqueous deposition (Zárate et al., Forthcoming). Siltstone intraclasts are scattered throughout the sedimentary matrix at some levels with very common carbonate nodules. Glass fragments are present throughout this upper section with the highest concentrations and largest pieces at the lowermost part, close to the boundary with the underlying siltstones. The entire exposure is capped by a thick calcrete crust up to 2 m thick, which in turn is overlain by upper Pleistocene and Holocene loess deposits. Fossil remains of vertebrates belonging to the Huayquerian South American Land Mammal Age (SALMA) have been recovered from these sediments (Deschamps 2003).

Glass fragments were also reported from Carhué, north of Sierra de la Ventana. Fossil remains exhumed from the outcrops in the surroundings of Bahía Blanca suggest a late Miocene Huayquerian age (Deschamps 2003, Deschamps personal communication). Eastward at the Las Oscuras site, recovered vertebrate assemblages indicate a younger age belonging to Montehermosan SALMA. A late Tertiary age was traditionally attributed to the sediments bearing glasses at Arroyo Claromecó, as well as the nearby locality of Arroyo Las Mostazas. Fossil remains collected at several localities along the Arroyo Claromecó valley (included in this study) were attributed to the “Irenense,” a unit correlated to the Montehermosan (Fidalgo et al. 1975).

CHARACTERISTICS AND COMPOSITION

Chasicó Glasses

The vesicular impact glasses from Chasicó resemble the Pliocene and Pleistocene samples, but there are significant

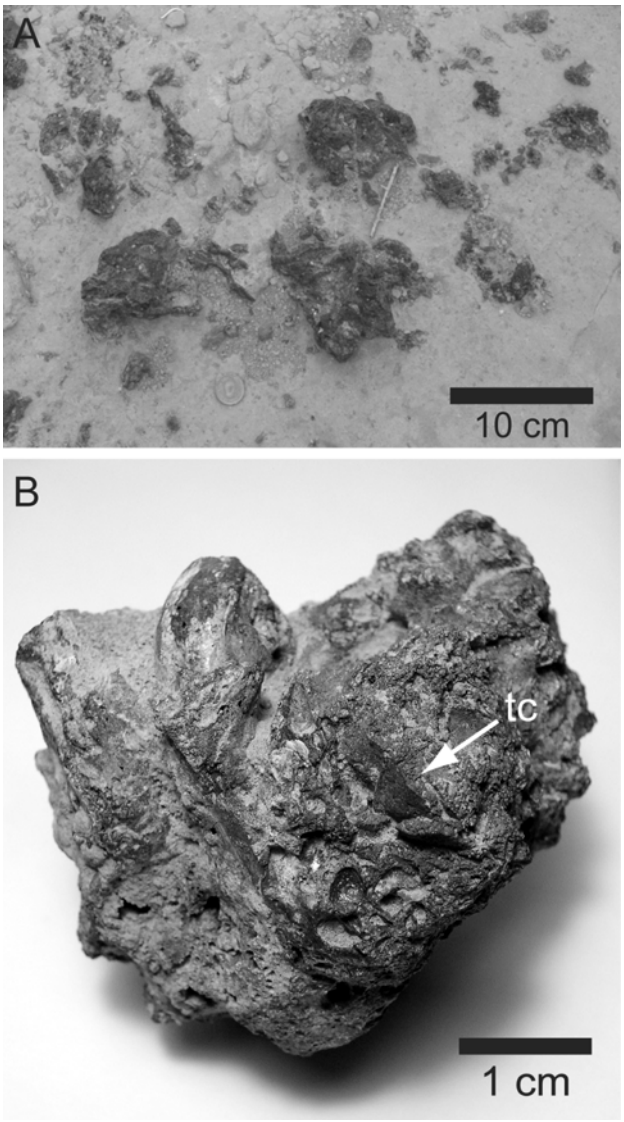

Fig. 2. Examples of Chasicó impact glasses. a) A photograph of an upper Miocene outcrop containing a large cluster of glasses. b) A close-up photograph of an individual clast of folded glass that contains a trapped tierra cocida (tc).

differences in the petrology and geochemistry consistent with their regional setting. The CH glasses exhibit large, twisted vesicles that occasionally contain seams of partially molten stringers of loessoid materials and are similar to the Rio Cuarto, Centinela, and Chapadmalalan impact melt breccias. But unlike the other glasses, CH samples are much darker, reddish-brown to brown (in hand specimen) glasses containing denser concentrations of quench crystals, typical of more proximal impact glasses.

The glasses range from centimeter-size fragments to 0.5 m diameter masses with some large clusters nearly 2 m across (Fig. 2a). Thin sections were made of seven different samples representing contrasting sizes (large versus small parent samples) and context (lower versus upper sequences). The mineral modes of unmelted xenocrysts (point counting averages from seven different thin sections) indicate plagioclase and K-feldspars as the most common (63 vol%) followed by Ca-pyroxenes (29 vol%), and quartz (28 vol%). The Ca-pyroxenes comprise a much greater fraction of unmelted minerals (factor of 2 to 5) than any other impact glasses from Argentina examined to date, excepting some of the BB samples.

The host sediments consist of both basaltic and andesitic rock fragments (40 vol%), volcanic shards (15–20 vol%), oligoclase-andesine plagioclase (25 vol%), and K-feldspars (~10 vol%). Heavy minerals (2–3 vol%) are represented by hornblende, augite, biotite, and opaques (in decreasing order). The petrologic composition of the sediments is generally consistent with the xenocrysts observed in the glasses, except for the lower fraction of quartz in the host sediments (<5 vol%) relative to the glasses (28 vol%). About half of the volcanic shards are in a weathered state but have not yet converted to clay. The Chemical Index of Alteration (CIA) for the bulk sediments is typically less than 50 (~46), which is consistent with a low degree of chemical alteration (Taylor and McLennan 1985).

Thin-sectioned glasses (CH-U, CH-U5) from the upper, reworked sediments exhibit little recrystallization with relict minerals comprising less than 5 vol%. Larger masses (CH-1, CH-G) underwent extensive recrystallization and relatively slow cooling rates, but still contain few relict minerals (<20 vol%). From the samples examined, glasses with the fewest mineral relicts and fastest cooling rates (based on crystal lengths) also were the most vesicular.

The bulk compositional range from XRF analyses (Table 1) indicates similar precursor materials (dacites, rhyolites, andesites, and trachytes) for some CH glasses. This would be expected for melting of bulk Pampean sediments derived from aeolian redistribution of fluvially transported materials from Andean source regions. Normative calculations cannot be used to characterize the source materials fully since impact glasses also contain foreign components (xenocrysts, melted clasts, and welded masses). Nevertheless, this strategy is useful for comparisons with other Pampean impact glasses and to explicitly identify possible contributions from sediments at depth.

The predominant glasses in certain samples (CH-1, CH-U5, and CH-U) have more basaltic compositions (basaltic andesite and trachytic basalt) relative to the rest of the glasses (Table 2). The different CH samples in Table 2 refer to different locations within the suite: CH-1, CH-W, and CH-G correspond to glasses from sediments lower in the section (CH-G and CH-1 from large samples); CH-U and CH-U5 are glasses from reworked sediments slightly higher in the section; and CH-Q is a sample from reworked sediments in a quarry about 50 km away from the primary exposures. All samples were collected within about 2 m of the lowermost occurrence in the section. Examination of Table 2 reveals no

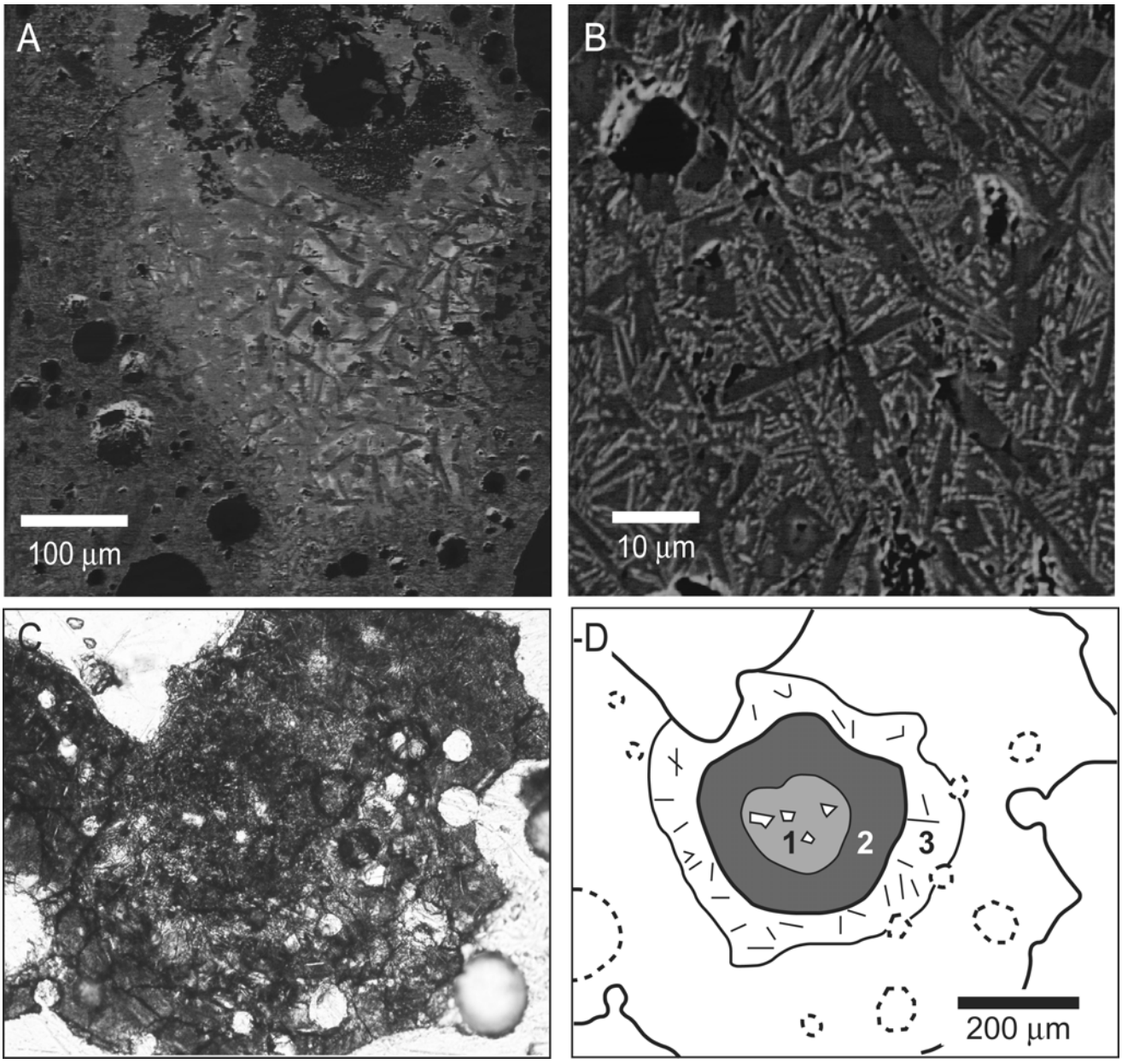

Fig. 3. a) A backscattered electron (BSE) image of basalt melt clast in Chasicó glass sample (CH-1). Crystallization appears to have occurred while the host mass was still plastic, e.g., undergoing aerodynamic flow (chilled margins, elongation). b) A BSE image showing host CH-1 glass with hyalophitic texture composed of skeletal (hollow and swallow-tail) plagioclase crystals with Mg-rich rims. c) A plane-polarized light photomicrograph (PPL) showing a basaltic melt spherule trapped within Chasicó impact glass (CH-1). d) A sketch illustrating the structure of the melt spherule. The dark core (regions 1 and 2) is composed of dense accumulations of very fine-grained, randomly oriented acicular crystals of Ca-pyroxene and plagioclase. Region 1 has a somewhat lighter appearance due to the presence of numerous tiny (and a few larger) feldspar xenocrysts. A rind (region 3) consisting of relatively clear quenched glass and sub-radially oriented plagioclase crystals separates the spherule from the host glass. The structure is similar to other xenocryst-bearing impact spherules found in the geologic record (e.g., Simonson 2003).

positive correlation between Al and Ca. Several Ca-bearing phases could account for the Ca: pyroxenes (or apatite as very small acicular crystals) from excavated continental basalts, additions from marine sequences, or carbonate nodules or cements. The high K_2O is attributed in part to the melting of K-feldspar-rich shards, which are abundant in the fine fractions.

Table 3 focuses on different portions of the CH glasses that are typified by Figs. 3a and 3b. These portions of the glass are normatively silica deficient and mafic enriched (diopside and hypersthene). Most CH samples contain abundant basaltic melt clasts (especially CH-1 and CH-W) composed of plagioclase and Ca-pyroxene quench crystals. These melt clasts have well-crystallized cores with grain sizes

Table 1. Major elements of bulk loess and bulk impact glasses.

	Host sed	Glasses					
	CH-LM	CH-1	CH-2	CH-A	CH-C	BB	RR
SiO_2	62.3	62.5	59.66	60.74	62.58	60.18	59.44
TiO_2	0.70	0.99	0.94	0.79	0.77	0.81	0.79
Al_2O_3	14.9	16.0	14.5	15.01	14.72	16.55	17.25
Fe_2O_3	5.55	5.74	6.09	5.69	5.95	5.75	5.60
MnO	0.005	0.004	0.05	0.02	0.02	0.11	0.10
MgO	3.82	2.37	3.24	2.87	2.64	2.69	2.62
CaO	5.55	4.18	6.97	5.27	4.92	5.58	6.71
Na_2O	4.32	3.4	3.71	4.24	3.79	2.88	2.66
K_2O	2.08	3.5	3.40	3.51	2.80	3.69	3.14
P_2O_5	0.17	0.38	0.75	0.54	0.84	0.51	0.77
Total	99.40	99.56	99.31	98.68	99.03	98.74	99.08
(LOI)	(11.52)	(4.31)	(3.28)	(4.79)	(3.86)	(2.20)	(5.17)

XRF data in wt% by C. K., University of Vienna; percentages exclude contributions from losses on ignition (LOI) given below. Abbreviations correspond to: Chasico (CH), Bahía Blanca (BB), and samples from a railroad cut (RR) near BB.

Table 2. Representative analyses of interstitial CH[a] glasses and BB[b].

	CH-G	CH-W	CH-U	CH-U5	CH-1	CH-Q	BB
SiO_2	64.9	60.8	62.3	64.9	62.1	65.8	62.0 (2.2)
Al_2O_3	12.0	17.1	19.6	16.4	14.4	16.8	15.4 (1.4)
TiO_2	0.76	0.87	0.92	0.68	0.76	0.74	0.78 (0.08)
FeO	8.6	6.65	5.0	3.65	4.6	4.4	4.5 (1.3)
MnO	0.25	0.23	0.15	–	0.08	0.12	–
MgO	2.32	3.15	2.20	1.45	3.21	2.27	2.3 (0.8)
CaO	8.35	5.4	4.05	3.15	6.1	4.2	5.0 (1.9)
Na_2O	1.25	3.25	1.8	3.80	4.15	2.21	2.9 (0.5)
K_2O	2.12	1.79	1.89	3.0	3.0	2.80	6.4 (0.9)
P_2O_5	0.58	0.67	0.45	0.13	0.29	0.33	0.66 (0.30)
Sum	100.13	99.91	98.36	97.16	98.74	99.67	99.94
BaO, NiO, Cr_2O_3 < 0.02%							
IUGS rock type[c]	Andesite	Dacite	Dacite	Trachyte	Dacite	Dacite	

[a]Electron microprobe analyses at Northern Arizona University (T. B. and J. W.).
[b]Electron microprobe analyses at the NSF/Keck Electron Microprobe Facility at Brown University (P. H. S.) with Na loss routine (Devine et al. 1995).
[c]Analyses normalized to 100% and calculated into normative components according to the International Union of Geological Sciences (IUGS) rock types.

Table 3. Microprobe broad beam analyses of CH series glasses (normalized to 100 wt%).

	CH-1		CH-G	CH-U5		CH-U		CH-W	CH-Q
	Quench	Dark		Clear	Dark	Clear	Flow		
SiO_2	62.7	53.2	60.5	60.0	62.3	60.1	57.9	60.6	70.0
Al_2O_3	16.0	16.0	19.5	12.4	18.3	16.1	11.8	17.5	15.4
TiO_2	0.87	1.19	0.78	0.66	1.24	0.98	0.61	1.04	0.37
FeO	3.65	5.1	2.89	2.92	2.73	4.5	3.36	4.05	1.86
MnO	0.08	0.06	–	–	–	0.05	–	0.04	0.12
MgO	2.36	3.4	1.7	2.98	2.07	2.60	4.3	2.63	0.91
CaO	6.9	14.0	5.7	9.9	4.2	5.5	9.7	4.8	1.72
BaO	–	–	–	0.19	–	–	0.25	0.03	0.12
Na_2O	4.75	3.68	5.0	5.5	6.3	3.42	3.8	5.0	3.81
K_2O	2.10	1.01	3.48	4.2	2.60	6.0	5.9	3.44	5.7
P_2O_5	0.66	2.36	0.45	1.26	0.26	0.75	2.38	0.57	0.50
Total	100.00	100.00	100.00	100.0	100.00	100.00	100.0	100.0	100.0
Totals (before normalization)	95.80	98.84	95.18	96.30	98.00	97.8	95.31	96.55	93.4

Electron microprobe data were performed at the Northern Arizona University (T. B. and J. W.). Low values before normalization are due to possible water and holes.

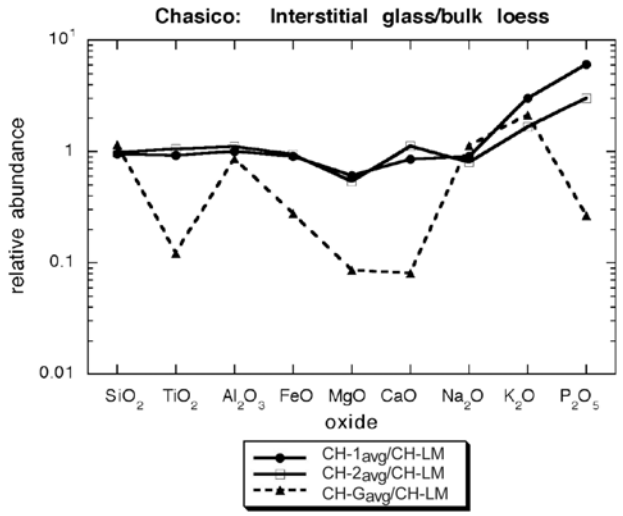

Fig. 4. The ratio of different interstitial averaged compositions (CH-1, CH-2, and CH-G) to bulk Miocene sediments (CH-LM). For the smaller Chasicó glasses, there is little difference between the interstitial glass and loess compositions. This reflects nearly complete melting during formation. CH-G is representative of larger CH masses which exhibit depletions consistent with incomplete melting of the target sediments.

decreasing toward the chilled margins (Fig. 3a). These clasts are surrounded by a melt with hyalophitic basalt textures (Fig. 3b). Figures 3c and 3d provide an example of another basaltic melt clast trapped in CH-1. Although most of these melt clasts have irregular to somewhat elongated shapes, a few (e.g., Figs. 3c and 3d) exhibit morphologies more typical of classic impact spherules (Simonson 2003). Basaltic textures include ophitic to subophitic, hyalophitic, variolitic, and intersertal. Maximum grain size in all cases is <7.5 μm with most at <4 μm. The microcrystalline basaltic components shown in Fig. 5 contain augite ($Fs_{14}Wo_{43}$) with mantles of hedenbergite ($Fs_{49}Wo_{51}$), plagioclase (An_{85}), and residual glass (FeO = 42 wt%). In addition, 0.48 wt% P_2O_5 was found in augite and 0.51% in the glass, perhaps from apatite in excavated basaltic materials or recently weathered by-products. Hedenbergite contains 0.13 wt% BaO and the glass has 0.15% BaO. Moreover, BaO was also found in the flow glass in CH-U (0.25 wt%) and the fractured glass in CH-U5 (0.19%). Such enhancements may represent the effects of hydrothermal processes.

Bulk analyses (Table 4) of the example shown in Fig. 3 show that the ophitic/subophitic core has an alkali basalt composition; the granular mantle, picrobasalt (olivine-bearing); and the chilled margin, andesite. The textures and compositional trends from core to chilled margin demonstrate rapid, in situ crystallization with compositional differentiation over very short distances. However, the crystallization rates are less rapid than those samples without such quench crystals as well as those samples that have quench crystals but little or no basaltic melt clasts. Other analyzed melt clasts are alkalic basalts and basaltic andesites.

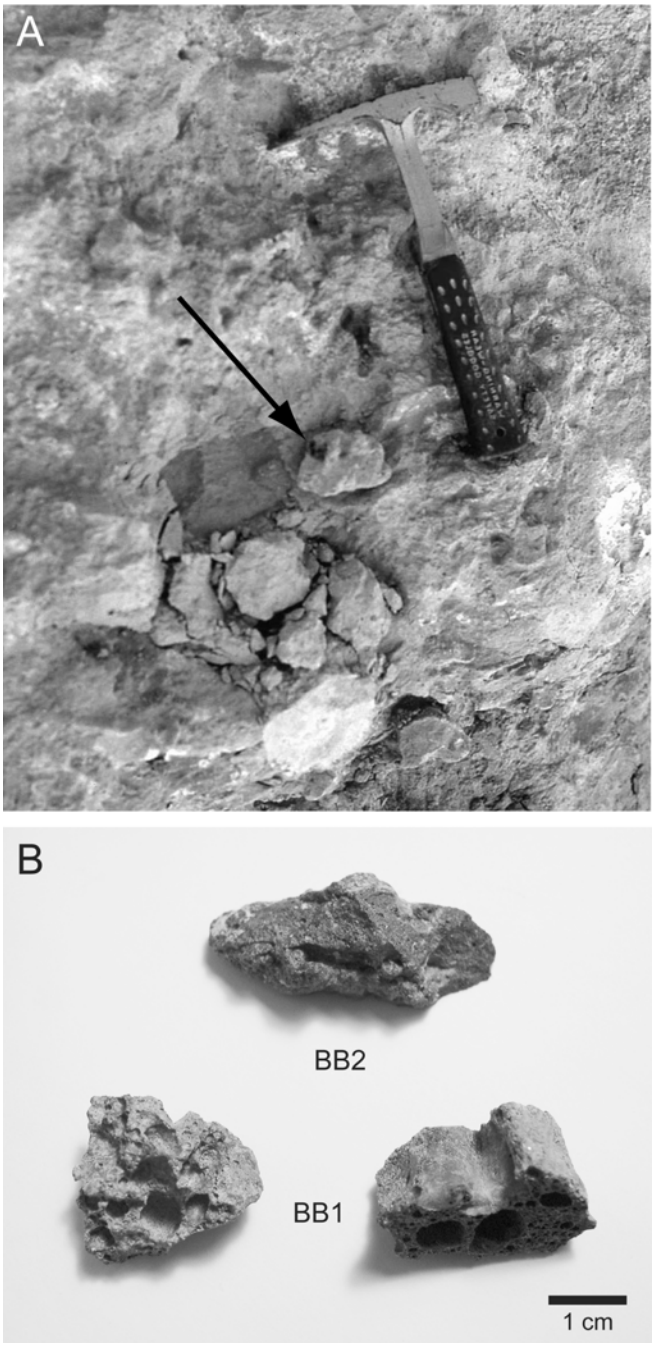

Fig. 5. Photographs showing examples of the small melt fragment (arrow) within a late Miocene, early Pliocene outcrop near Bahía Blanca (a). Similar glass fragments occur throughout the upper Miocene to lower Pliocene sections within 500 km of Bahía Blanca. Examples of extracted glasses are shown in (b).

The low totals in Table 3 are largely due to vesicles included in the broad-beam analysis.

The major element composition of the CH glasses generally resembles the post-Miocene Argentine impact glasses consistent with generally similar precursor materials (i.e., loess derived from Andean volcanics), but there are also significant differences. Figure 4 provides a plot of the

Table 4. Microprobe broad beam analyses of inclusions in impact glass from Chasico (CH-1).

	Subophitic core	Melt clast 1 (Fig. 3a) granular mantle	Chill margin	Melt clast 2	Melt clast 3
SiO_2	45.7	44.7	59.8	54.0	50.2
Al_2O_3	12.8	13.3	16.4	17.0	18.7
TiO_2	1.0	0.96	0.97	1.0	0.78
FeO	6.4	3.77	3.65	5.8	3.80
MnO	0.26	0.10	0.05	0.05	0.07
MgO	7.4	9.7	3.13	2.97	5.7
CaO	22.8	24.3	9.2	12.7	17.5
BaO	–	0.10	0.13	–	–
Na_2O	0.94	0.36	4.55	4.0	2.48
K_2O	0.18	0.08	1.50	1.11	0.27
P_2O_5	2.52	2.63	0.57	0.42	0.55
Totals	100.0	100.0	100.0	100.0	100.0

Electron microprobe data were performed at the Northern Arizona University (T. B. and J. W.).

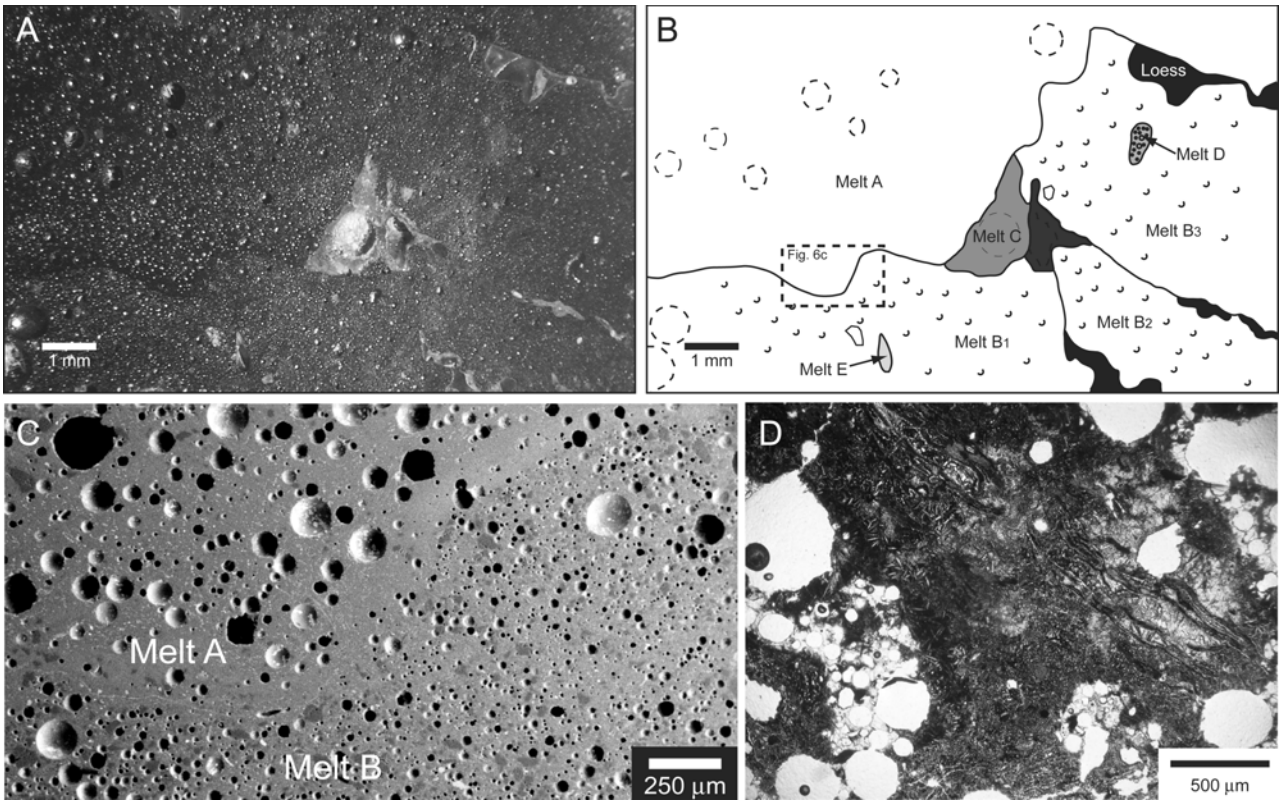

Fig. 6. a) A reflected light photomicrograph of a literal impact melt breccia (i.e., composed of multiple distinct melt clasts in contrast to lithic clasts set in a melt matrix) from BB2 (polished thin section). b) A sketch of (a) showing the locations and relationships of different melts and loess stringers. Melt A is black, smooth, and enriched in Ca, Ti relative to Melt B, and also contains fewer small vesicles and fewer clasts. Melt B is red and contains abundant small vesicles and clasts. Melt C is a sulfur-bearing melt that was originally a soil or similar material associated with loess and trapped along same seams as loess stringers. Melt D is a K, Fe-rich vesicular melt with abundant unmelted quartz and magnetite grains. Melt E is a silica melt, probably a lechatelierite particle. c) A BSE image of the boxed region in (b) showing the sharp seam between Melt A and Melt B. d) A PPL photomicrograph of a melt-rich suevitic breccia from BB1. Distinct vesiculated or flow-banded glass clasts are set in a fine-grained, clast-rich matrix.

interstitial clear and bulk glass composition from microprobe analyses ratioed to the bulk sediment composition in which they occur. While most of the major elements of the smaller (<5 cm) glasses closely resemble the host sediments, K_2O and P_2O_5 levels are clearly enriched. Analysis of a very large (0.5 m in diameter) impact melt breccia (CH-G), however, reveals significant depletions in TiO_2, FeO, MgO, and CaO, probably reflecting incomplete melting of refractory oxide minerals. Aqueous alteration, possibly hydrothermal, is likely responsible for the observed enrichment in K_2O.

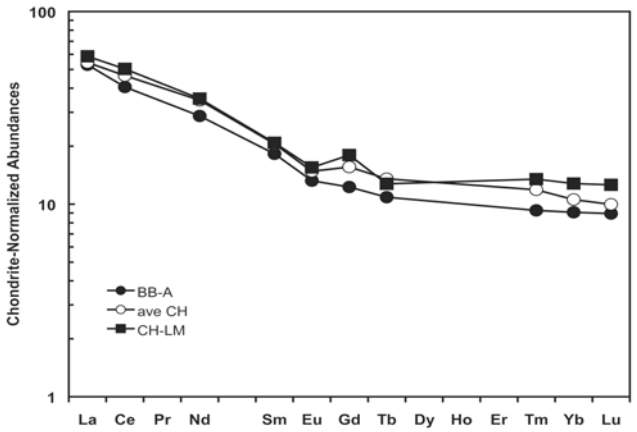

Fig. 7. Distribution of rare earth elements (REE) for average CH glasses (open circles), BB glass (filled circles), and host CH sediments (filled squares). The impact glasses exhibit a smaller Eu anomaly consistent with a source more mafic than the host sediments.

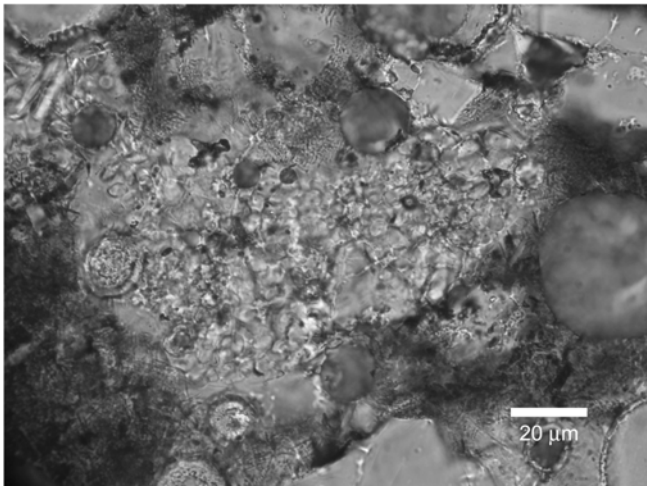

Fig. 8. A PPL photomicrograph of a polycrystalline quartz grain in CH glass that exhibits ballen texture.

Bahía Blanca Glasses

The Bahía Blanca glasses (e.g., Fig. 5) generally occur as small (<5 cm) pods of grayish to black materials, some of which do not resemble glasses at first glance, except where vesicles are conspicuous (e.g., two specimens from BB1 in Fig. 5). The BB-2 specimens tend to appear black and dense both on weathered and polished surfaces (Fig. 6). As discussed above, BB glasses occur in Miocene units covering a wide region, including the RR sample. Tables 1 and 2 provide data indicating that the BB and RR samples have bulk and interstitial glass compositions resembling the glasses from Chasicó.

More than twenty thin sections and polished SEM mounts were made from a dozen small glasses collected in the vicinity of Bahía Blanca. The glasses exhibit tremendous compositional and textural variability, especially for the small number of specimens collected from only a few sites. Nearly every classification of impact melt is present including clast-poor and clast-rich melt-matrix breccias similar to the Chasicó glasses, literal impact melt breccias (composed of multiple, distinct melt-rich clasts) (Figs. 6a–c), pieces of suevitic breccias (Fig. 6d), and even some gradational forms. Because of this wide range, a full description of these materials will be deferred to a later contribution. Here the focus is to provide a basic description and sufficient petrography to establish their impact origin.

Geochemistry

The CI-normalized distribution REE, shown in Fig. 7, indicates that the CH and BB glasses are reduced in the light REE relative to the Miocene sediments. Certain minor elements in the CH glasses (Table 5) exhibit significant differences from the host sediments. The most significant difference is the order of magnitude increase in Ba, from a nominal level of less than 400 ppm (matrix) to as high as 7600 ppm (CH-1 glass). As noted in the petrography and microprobe data, BaO was found in the flow glass of two samples (exhibiting evidence of hydration) and within hedenbergite mantles around augitic cores. The selected elements that are more indicative of provenance also contrast with the host sediments. For example, the impact melts exhibit slightly more mafic affinities (V, Sc, La, and Th) than the host sediments as well as reduced concentrations of REE. Other ratios (K/U, Zr/Hf, Hf/Ta, and Th/U) also indicate that the impact glasses incorporated more mafic material than those in the host sediments. Consequently, the CH glasses indicate that the impact may have penetrated a basaltic flow and/or was then subjected to hydrothermal alteration.

SHOCK PETROGRAPHY

Chasicó Glasses

Impacts into porous sedimentary targets, such as the thick Pampean sediments, are not expected to efficiently transfer the energy of the shock wave to the mineral grains (e.g., Grieve et al. 1996) due to the low impedance of the pore spaces between them. Instead, a significant portion of the energy is consumed by collapsing pore-space and compressing grain boundaries, thereby producing copious heat in the target materials (Kieffer 1971). Consequently, sedimentary targets typically experience extensive melting at much lower pressures than crystalline targets (Kieffer et al. 1976; Stöffler 1984). Many grains, therefore, probably never experience sufficiently high pressures to either produce planar deformation features (PDFs) or initiate other solid-state transformations. The small number of grains that do record high pressures are likely melted soon thereafter (French 1998). The odds of finding shocked mineral grains in

Table 5. Trace element geochemistry of Miocene impact glasses.

	CH-1	CH-2	CH-A	CH-C	BB-A	RR-1	CH-Sed	MdP-Sed
V	120	119	110	107	128	114	93	116
Sc	12.1	15.2	13.4	13.9	14.8	13.6	13.9	12.9
Cr	28.7	23.9	34.1	30.7	46.6	88.3	30.3	29.1
Co	7.58	9.05	9.17	10.1	13.5	11.6	8.42	10.5
Ni	5	6	10	10	20	25	9	25
Cu	3	<2	<2	6	27	36	<2	31
Zn	23	32	22	49	31	25	60	80
Ga	30	60	5	20			20	
As	8.43	6.72	3.48	3.97	2.9	2.7	7.57	3.1
Se	0.6	0.6	0.8	0.9	0.4	0.1	0.7	0.4
Br	0.9	2.2	3.2	5.9	0.4	8.5	19.1	28
Rb	66.5	43.9	71.3	70.1	58.1	54.8	69.2	73.4
Sr	471	585	493	424	430	546	371	287
Y	24	29	27	30	24	26	28	21
Zr	176	157	162	163	164	178	159	220
Nb	10	8	9	9	12	11	9	14
Sb	0.26	0.29	0.08	0.31	0.37	0.31	0.34	0.62
Cs	4.03	2.33	4.41	4.64	3.29	3.10	5.04	4.62
Ba	7693	2391	1745	613	562	445	374	395
La	20.1	20.4	18.8	20.5	19.4	18.7	21.5	22.7
Ce	39.7	43.8	44.2	50.2	38.8	35.5	48.2	48.1
Nd	21.1	25.9	25.4	26.1	20.4	19.5	25.1	26.4
Sm	4.31	5.44	4.17	5.07	4.21	4.16	4.81	5.21
Eu	1.08	1.40	1.26	1.41	1.15	1.19	1.35	1.25
Gd	4.2	5.2	4.5	5.2	3.75	3.47	5.5	4.37
Tb	0.67	0.79	0.76	0.92	0.63	0.65	0.74	0.76
Tm	0.38	0.43	0.41	0.47	0.33	0.34	0.48	0.39
Yb	2.39	2.94	2.46	2.69	2.25	2.29	3.17	2.76
Lu	0.35	0.41	0.35	0.41	0.34	0.35	0.48	0.43
Hf	4.55	4.35	4.82	4.52	4.11	4.18	4.69	5.38
Ta	0.43	0.33	0.55	0.48	0.44	0.42	0.65	0.57
W	0.8	1.5	0.5	0.6	0.7	0.9	1.5	1.1
Ir (ppb)	<1	0.1	0.4	<1	<0.7	<0.9	0.2	<0.5
Au (ppb)	5	8	3	<8	1.1	0.5	<5	0.2
Th	6.42	5.32	7.18	7.23	6.12	5.75	7.41	7.90
U	1.99	1.61	1.22	1.02	1.65	1.39	2.25	1.58

C. K., University of Vienna, XRF and INAA data; trace elements in ppm, except as noted. CH stands for Chasico; BBQ stands for Bahía Blanca; RR stands for distal glass probably related to BB; CH-Sed and MdP-Sed stand for host sediments for impact glasses at Chasico and Mar del Plata.

the melt products of impacts into the Pampean sediments are then reduced even further by the very small size of the surviving crystals. Hence, the chances of discovering shocked quartz are diminished by the extreme paucity of quartz in many of the strata.

The seven Chasicó thin sections discussed above (along with numerous paired sections) were examined using optical petrography and scanning electron microscopy (SEM) for any evidence of high pressure/high strain rate deformation, high pressure/high temperature phase decomposition, or very high temperature melting that is either indicative or suggestive of impact processes. While more complete results will be reported in future contributions, the most significant findings are presented here to establish the impact origin of the 9.2 Ma Chasicó glasses.

Initial observations revealed abundant tapered to droplet-shaped polycrystalline grains (<100 μm) interpreted to be recrystallized potassium feldspars and quartz. The recrystallized quartz grains (Fig. 9) commonly exhibit the “ballen” texture first described by Carstens (1975) as a reversion product from diaplectic glass. When ballen quartz forms after lechatelierite, it typically exhibits the polycrystalline habit, inhomogeneous extinction (Bischoff and Stöffler 1984), and occasional vesiculation (Stöffler and Langenhorst 1994) that is observed in the Chasicó grains (Bischoff and Stöffler 1984). Lechatelierite may form as a result of shock pressures exceeding 50 GPa (Stöffler and Langenhorst 1994) or temperatures exceeding 1700 °C. In naturally occurring rocks, therefore, lechatelierite is indicative only of impact metamorphism or lightning strikes (Montanari and Koeberl 2000). Given the morphology, size, apparent volume, and geographic extent of the glasses

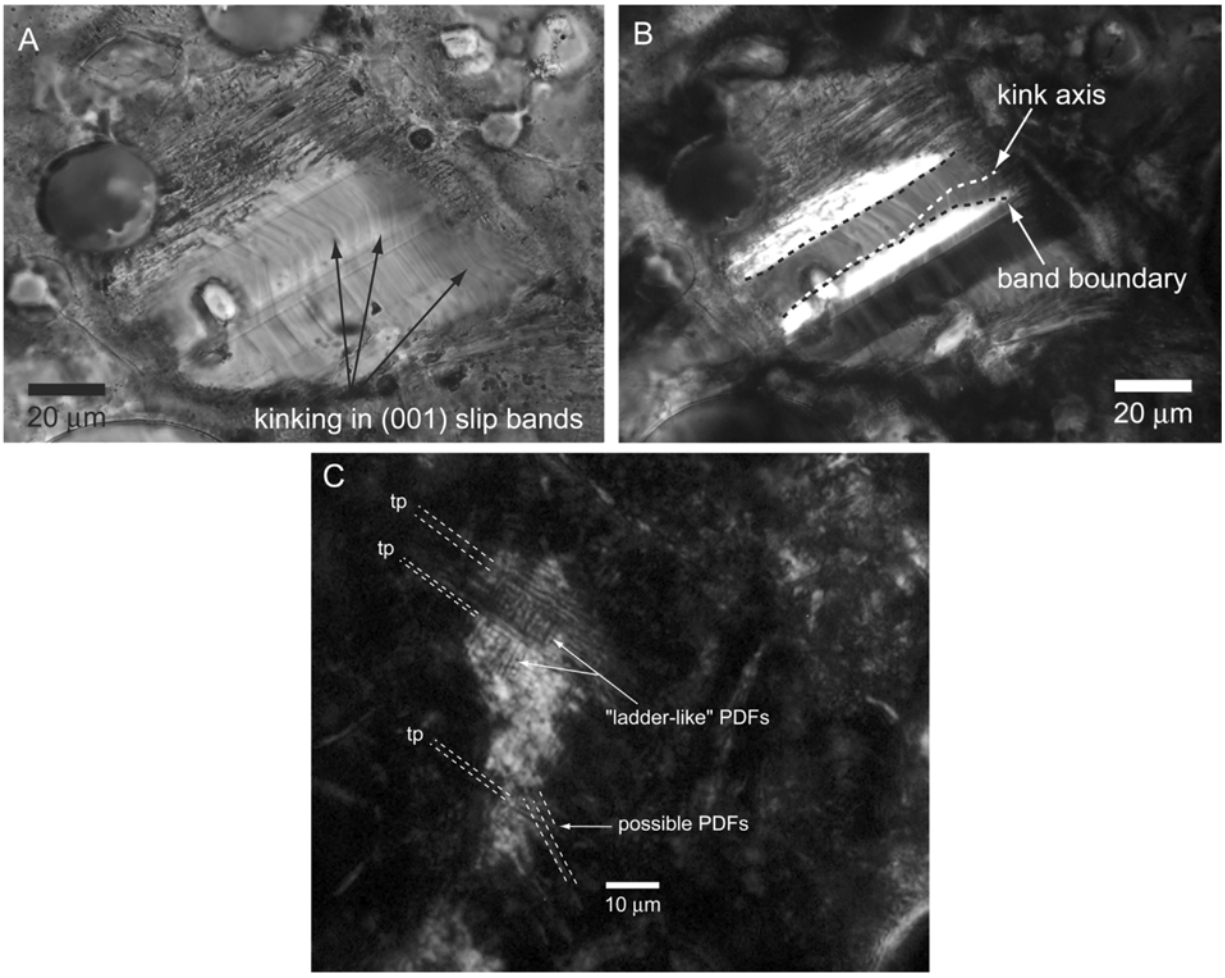

Fig. 9. a) A PPL photomicrograph of a kink banded plagioclase grain in CH glass showing narrow, parallel isotropic slip bands trending NW-SE through the grain. The slip bands are deflected across a set of kink bands oriented SW-NE. b) A cross-polarized light (XPL) image reveals the boundaries between each kink band. In one kink band (center), the axis of inflection diverges from the band boundary, which may indicate some shearing following the rotation of the lattice. c) An XPL photomicrograph of a partially altered shock-metamorphosed plagioclase grain within a CH glass showing the distinct "ladder texture" (e.g., Stöffler 1966; French 1968) formed by sets of closely spaced PDFs stacked like rungs between albite twin planes (tp).

(coupled with the additional evidence of impact process discussed below), it is most reasonable to conclude that these grains represent shock melted droplets of quartz and feldsparthat became entrained in the glasses during excavation and ejection from the impact site.

Evidence for a wide range of shock metamorphic conditions are found among the abundant unmelted plagioclase grains in the CH thin sections. In general, shock indicators are observed in less than 20 grains per thin section. These numbers increase steadily as each section is reexamined as a consequence of searching grain of minute size, which are in close contact with arrays of tiny quench crystals. Some plagioclase grains (Fig. 9a) contain prominent kink banding corresponding to relatively low pressure/high strain rate formation. Although kink bands also can occur in tectonically deformed rocks (though rarely), they are common in impactites (Bunch 1968). Smith and Brown (1988) list their association with closely spaced, isotropic slip bands as a characteristic of naturally shocked feldspars. Von Engelhardt and Stöffler (1968) refer to this type of deformation as "a typical criterion for shock damage."

Moderately high shock conditions are evidenced by the formation of PDFs in plagioclase. The most obvious PDFs are those that form the "ladder texture" (Fig. 9b) first described in detail by Stöffler (1966) from twinned plagioclase grains in Ries suevites. Short incipient or relict PDFs with multiple orientations are also observed within the crystalline regions of other plagioclase grains which have undergone a peculiar type of transformation apparently unique to impact metamorphism (Fig. 9b). "Alternate twin melting" (Reimold et al. 2004) or "asymmetric isotropization" (Dressler 1990) is a phenomenon also first described by Stöffler (1966) in plagioclase grains from the Ries. This style of deformation results in the formation of diaplectic feldspar glass but only within albite

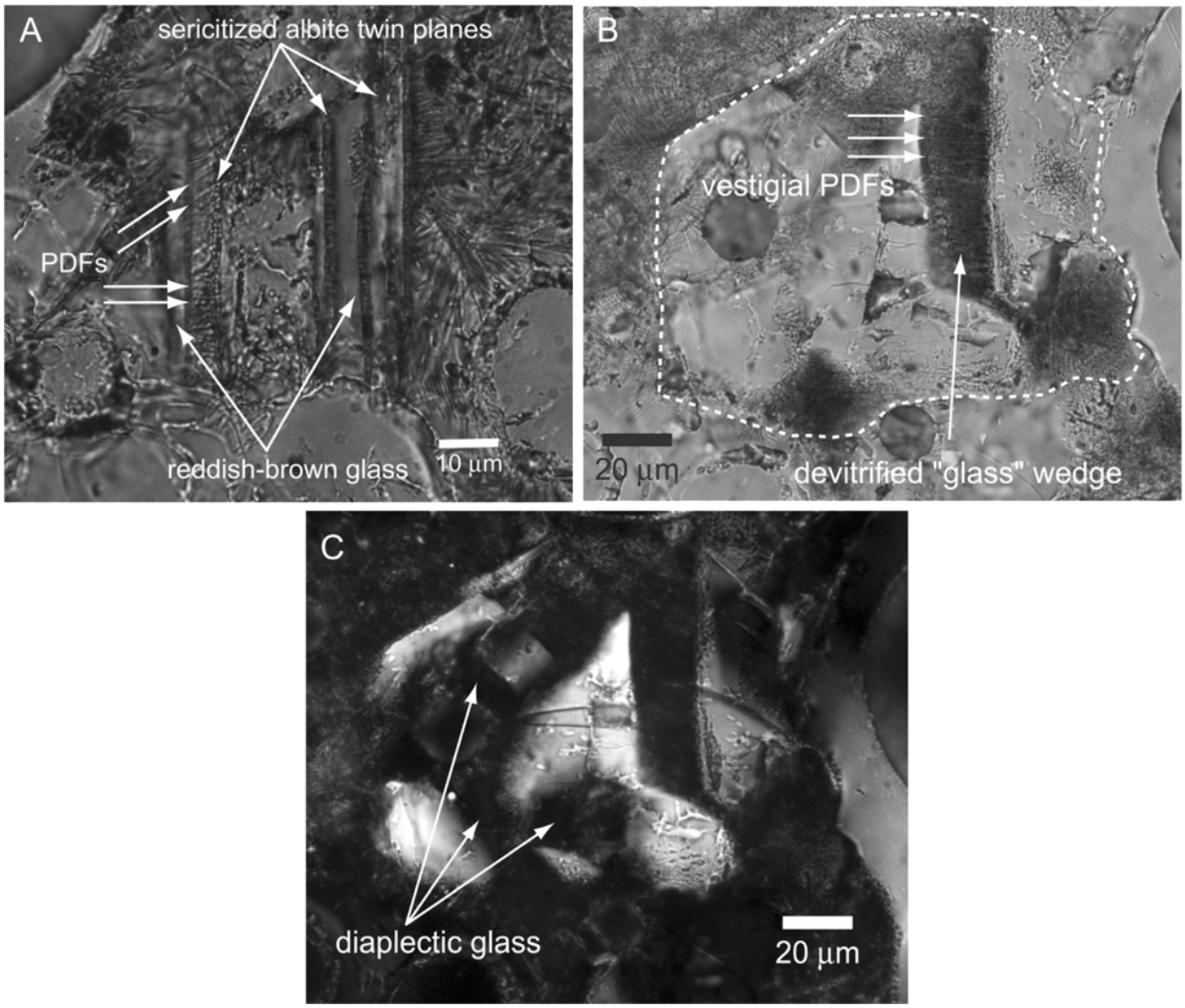

Fig. 10. a) A PPL photomicrograph of shock-metamorphosed plagioclase grain within a CH glass. The grain exhibits a pattern similar to the amorphitization of alternate albite twins first noted by Stöffler (1966) in shocked plagioclase grains from the Ries crater. In the original section, the glass twins have a distinctive reddish-brown hue. b) PPL and c) XPL photomicrographs of a shocked plagioclase grain within a CH glass. Irregular isotropic patches occur where the grain has been partially converted to diaplectic glass. Note that the relatively weak glass has preferentially been removed during grinding, leaving several holes. A wedge-shaped zone of partially devitrified glassy material extends into the top of the grain. This zone may have been densely packed with PDFs, the outlines of which appear to be preserved despite some recrystallization.

twins of a particular set (typically ever other twin). This is believed to occur because the lattice of each twin in a given set is rotated some equal number of degrees, relative to the intervening set, thereby causing one set to have an orientation relative to the shock wave more favorable for the disordering of the crystal. The "surviving" twin set commonly will contain PDFs (Stöffler 1966), but the exact pattern can become quite complicated, depending on the original rotation of each twin (Dressler 1990). The pattern illustrated by the grain in (Fig. 10a) might be the result of the original complexities in lattice orientations, but it also might have resulted from perturbations in the shock wave induced by pre-existing clay minerals lining the twin planes of the weathered feldspar. The reddish-brown coloration of the amorphous twins (in the original section) is similar to the "altered alternate albite twin" effect discussed by Short and Gold (1996) as a signature of shock metamorphism in rocks from the Manson structure.

The most common shock features of CH plagioclase grains include the irregular isotropic patches of reduced refractive index interpreted as zones of diaplectic glass, or maskelynite (Fig. 10b). Commonly these grains also contain distinct broad, wedge-shaped domains that appear to invade from the crystal margins. These features appear similar to the L2 isotropic lamellae characterized by White (1993) at the Manicouagan structure. Like the L2 lamellae, such features in Chasicó plagioclase grains also seem to be associated with dense arrays of PDFs.

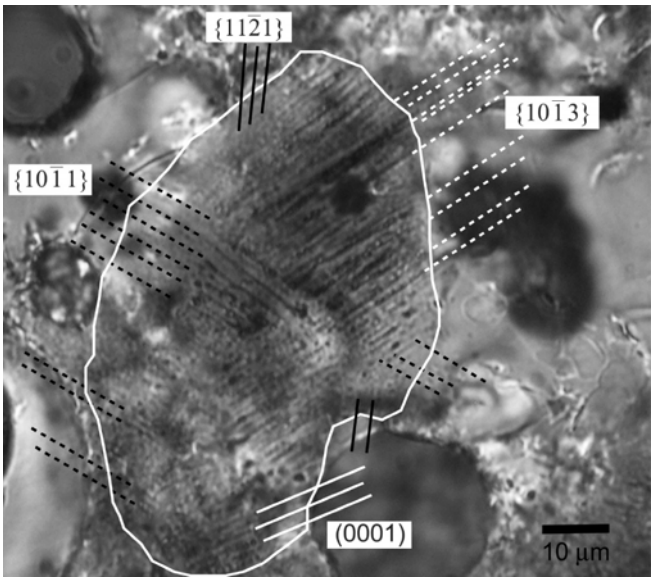

Fig. 11. A close-up PPL photomicrograph of a shocked quartz grain, one of five grains that comprise a shocked quartzite fragment found in CH-W. The grain contains at least five sets of decorated PDFs. The decoration consists of extremely straight chains of minute fluid inclusions. Four PDF sets are observable in the shown orientation; the fifth set, parallel to {10$\bar{1}$3}, is seen with the U-stage upon tilting the thin section.

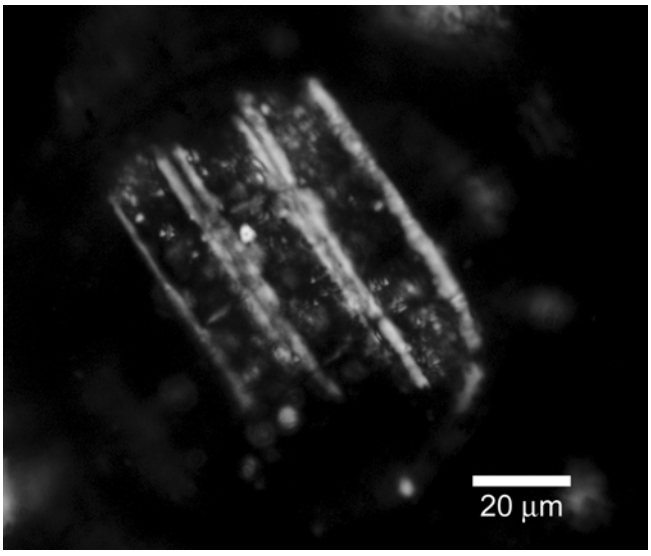

Fig. 12. An XPL photomicrograph of a shocked plagioclase grain embedded in impact melt breccia from BB2. Every other albite twin has been converted to an amorphous, isotropic phase. Note that within that set of diaplectic twins, every other member of the set appears to have been compressed. This same pattern is observed in shocked plagioclase grains from other established impact sites (e.g., Stöffler 1966). The large isotropic twins also exhibit a reddish-brown hue in PPL.

The search for shocked quartz thus far has identified six grains containing one or more sets of decorated PDFs and exhibiting the common "toasted" coloration as detailed by Whitehead et al. (2002). Of the six, five grains are part of the same tiny (~500 µm) angular quartzite fragment. Unfortunately, the extinction pattern of only one grain (Fig. 11) is regular enough to facilitate indexing the planes according to established techniques using the Universal stage (Engelhardt and Bertsch 1969). The grain contains decorated PDFs along five crystallographic planes corresponding (± 4° error) to (0001), {10$\bar{1}$3}, {10$\bar{1}$1}, {11$\bar{2}$1}, and {10$\bar{1}$0}. If the quartzite clast containing this grain is derived from crystalline rocks at depth, these PDF orientations are indicative of shock pressures between 12 and 20 GPa (Stöffler and Langenhorst 1994).

Bahía Blanca Glasses

The same mineral shock indicators recognized in the Chasicó glasses are present in the Bahía Blanca glasses; therefore, only supplemental examples are provided here. Figure 12 shows a classic example of asymmetric isotropization, or alternate twin melting, which is indicative of crystallographically controlled generation of diaplectic glass under shock pressure. Lechatelierite (Fig. 13a) is indicative of temperatures exceeding 1700 °C (e.g., Hudon et al. 2002) or shock pressures greater than at least 50 GPa (e.g., Stöffler and Langenhorst 1994). The partially molten rutile grains (Fig. 13b) indicate more extreme temperatures (>1847 °C) (El Goresy 1968). Additional consequences of shock loading in BB grains include well-developed planar fracturing/faulting in quartz (Fig. 14), as well as diaplectic quartz (Figs. 15a and 15b), and diaplectic feldspar (Figs. 15c and 15d). Quartz grains exhibiting pronounced isotropization, planar fracturing/faulting, or mosaicism typically show reduced refractive indices and birefringence and contain one or more sets of generally faint, often discontinuous planar fluid inclusion trails that probably represent decorated and partially annealed PDFs. Other likely shock products observed include "ladder-like" PDFs in plagioclase, checkerboard K-feldspar, microtwinning in ilmenite, well-developed planar fracturing and microfaulting in olivine, and intense microtwinning in clinopyroxene. The details of these features will be reported in a future contribution.

RADIOMETRIC AGE

Four different $^{40}Ar/^{39}Ar$ age determinations for glasses from the Miocene loessoid sections from Chasicó and Bahía Blanca were made. All samples were analyzed using laser incremental heating methods and noble gas mass spectrometry at the Berkeley Geochronology Center as described in Renne et al. (1998). Data for these samples were evaluated with the statistical program described by Sharp and Deino (1996). Glass samples were prepared for irradiation by gently crushing with a ceramic mortar and pestle, followed by hand picking of about 100–200 mg with a petrographic microscope to minimize the effects of alteration, xenocrysts,

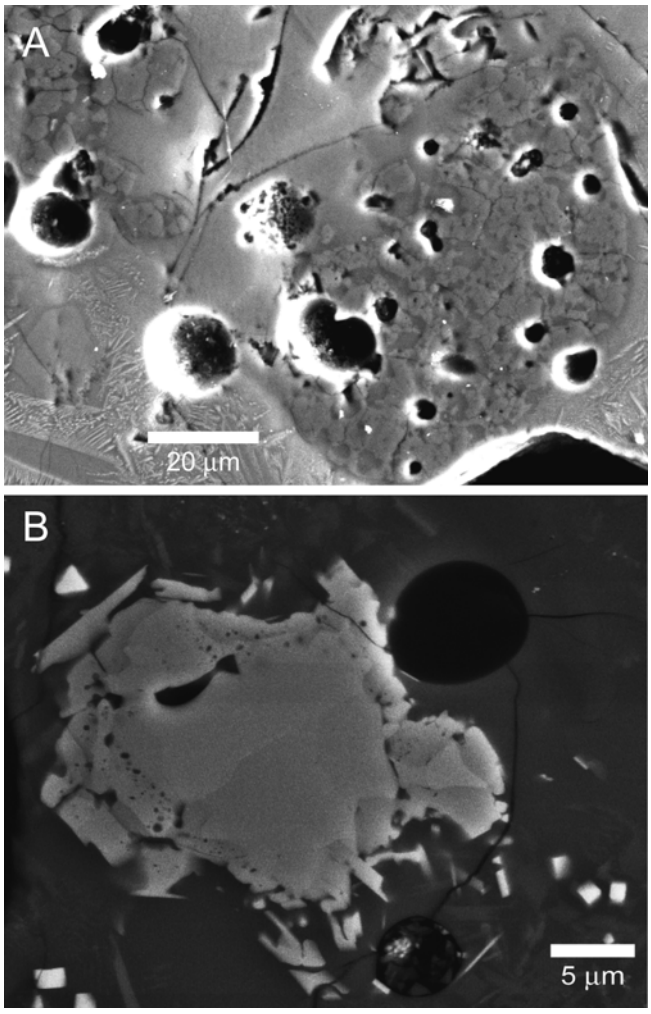

Fig. 13. Evidence for extremely high temperature melting in Bahía Blanca glasses. a) A BSE electron micrograph showing a vesiculated grain of fused quartz (lechatelierite), which is indicative of temperatures exceeding 1700 °C. Lighter gray portions of the grain are pure SiO_2, while darker regions represent infiltration of ions from the surrounding melt along cracks in the silica glass. These regions are slightly enriched in magnesium, sodium, and aluminum (and likely water) with lesser concentrations of potassium, iron, and calcium. b) A BSE image of an embayed, partially melted rutile grain providing evidence that BB impact melts locally achieved temperatures exceeding ~1850 °C (El Goresy 1968).

and vesicles. Following irradiation, about 10–20 mg of material was selected through a final inspection for incremental heating analysis.

Two age determinations were made for different samples from Chasicó (Fig. 16a). These samples were selected from lower (CH-L, paired sample with CH-1 glass) and upper reworked sediment layers (paired sample with CH-U) as described in the section on geologic setting. The glass for each of the Chasicó samples was dark brown and relatively fresh, similar to the glasses from Bahía Blanca. Sample CH-L yielded an incremental heating spectrum with initial release of non-atmospheric, extraneous ^{40}Ar in the first step,

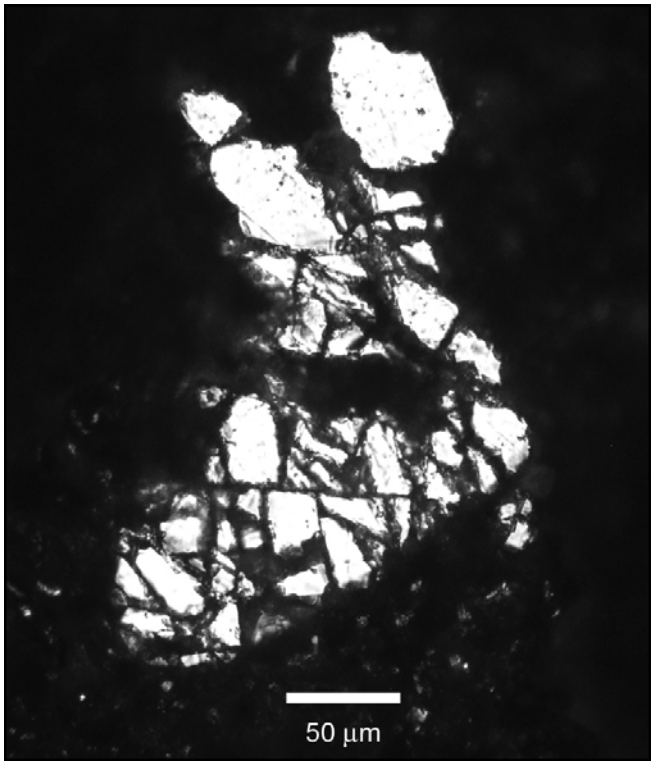

Fig. 14. An XPL photomicrograph showing extremely well-developed planar fracturing in quartz. Note that the N-S trending cleavages are displaced along those trending E-W (basal planes), indicating microfaulting that must have been synchronous with production of the host melt. Otherwise, the resulting sharp edges along the grain margin would have been weathered away.

followed by three steps with ages of ~9.20 Ma, and finally by decreasing age in the highest temperature steps. The decreasing age of the highest temperature steps appears to be the result of some minor contamination from a calcic phase (carbonate or plagioclase), but it appears to have little effect on the overall age spectrum. A plateau age for the sample of 9.23 ± 0.09 Ma is defined by the first four heating increments and 87% of the ^{39}Ar released. Because the radiogenic yields for the main steps of the heating analysis are uniformly about 95%, there is little spread of the data, and the data do not define an isochron. Regression of all the data for this sample yields an age similar to that defined by the plateau, and an "initial" $^{40}Ar/^{36}Ar$ ratio of 314 ± 16 (that is controlled mainly by the first analysis). The incremental heating data for sample CH-U are very similar, with a plateau age of 9.3 ± 0.3 Ma. The radiogenic yields for heating steps of CH-U are generally lower than with CH-L, thereby producing a higher uncertainty and suggesting a greater degree of glass alteration. This interpretation is consistent with the stratigraphic context indicating deposition of reworked sediments and glasses for the upper deposit.

The glasses from Chasicó are interpreted as the same age. Due to the statistically identical results and relative uncertainties, the preferred weighted average of 9.24 ±

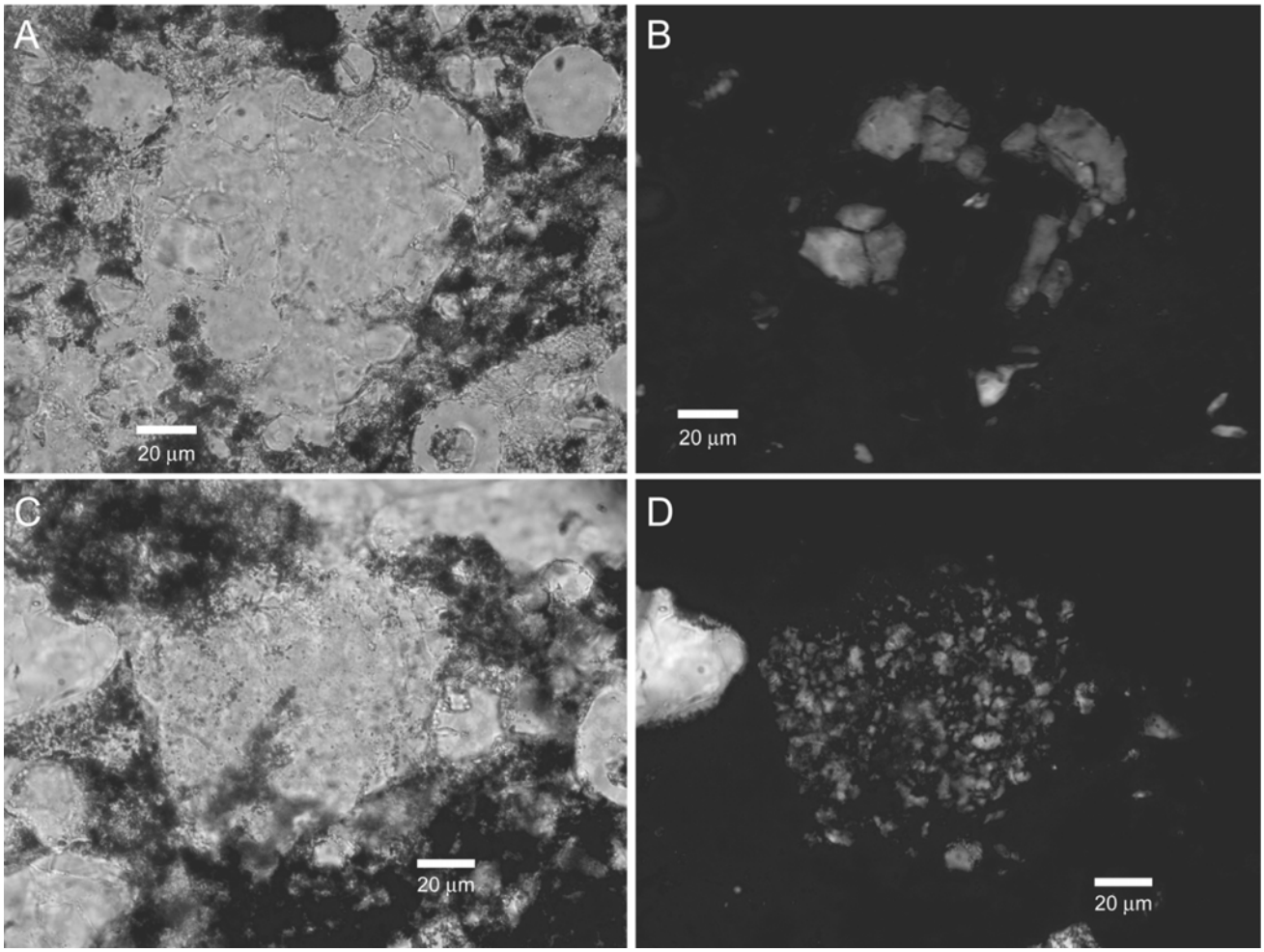

Fig. 15. Shock effects in Bahía Blanca quartz and feldspar. a) PPL and b) XPL photomicrographs of quartz grain containing broad regions, characterized by reduced refractive indices and isotropy, interpreted to be diaplectic glass. c) PPL and d) XPL photomicrographs of feldspar grain showing extensive recrystallization inside well-preserved grain boundaries indicative of either diaplectic feldspar or fused feldspar that quenched sufficiently quickly to prevent flow and deformation of the original grain boundary. Either explanation requires impact shock processes (French 1998).

0.09 Ma is adopted as the timing of the Chasicó glass formation. An earlier publication cited a preliminary age of about 10 Ma (with larger uncertainties) for the Chasicó glasses from the same exposure (Schultz et al. 1999) based on analyses in another laboratory. The glasses from Chasicó analyzed in the present study, however, are superior in quality and quantity to the material previously analyzed. Moreover, the techniques employed in this study are considered superior for the resolution of extraneous argon, and thus the age of 9.24 ± 0.09 is now preferred.

Two glass samples were analyzed from exposures near Bahía Blanca. The glass for each sample was relatively fresh and free of xenocrysts, although vesicles were conspicuous throughout. The $^{40}Ar/^{39}Ar$ incremental heating release spectra of these samples (Fig. 16b). are characterized by release of extraneous atmosphere-rich argon (low radiogenic yields) in the initial heating steps, followed by increments with ages of ~5.2–5.3 Ma that have radiogenic yields of 80% or greater. Plateau ages for samples BB-1 and BB-2 are 5.32 ± 0.05 Ma and 5.24 ± 0.05 Ma, respectively. Since there is considerable spread in their atmospheric argon contents, each sample defines an isochron; the $^{40}Ar/^{39}Ar$ ratio indicated for the trapped argon in BB-1 is 297.3 ± 1.6, and for BB-2 it is 298.7 ± 1.2. As these ratios are very near that of modern atmospheric argon and the higher-temperature release steps are fairly radiogenic, the isochron ages are identical to the plateau ages. Our preferred assessment of the formation age for glass from Bahía Blanca is 5.28 ± 0.04 Ma, obtained by averaging the plateau ages.

DISCUSSION

The radiometric dates and stratigraphic placement establish two different layers of impact glasses. The 9.2 Ma

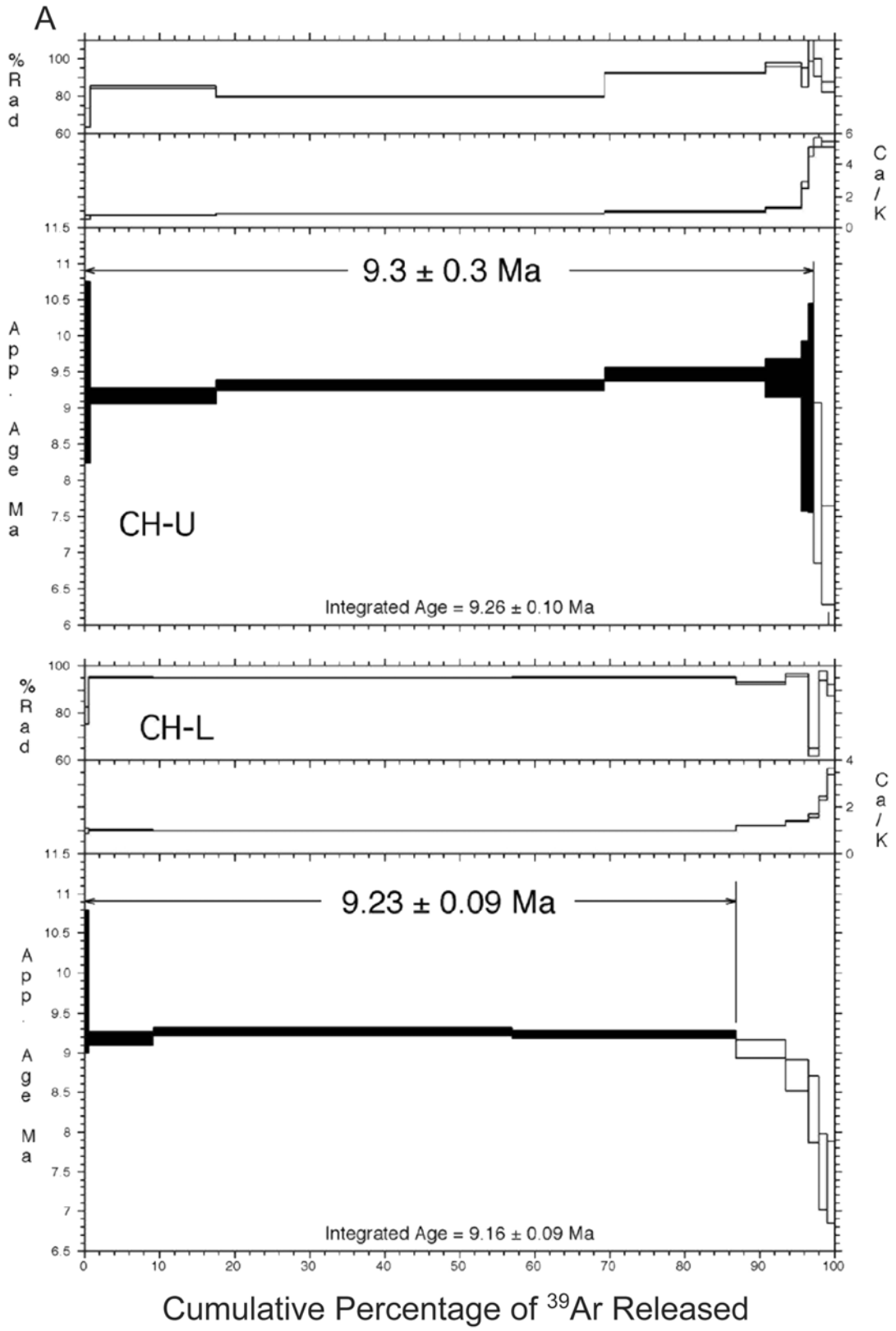

Fig. 16. a) $^{40}Ar/^{39}Ar$ incremental heating spectra for clast-free fractions two Chasicó impact glasses. Ch-U corresponds to material from reworked deposits slightly higher in the section than CH-L. The plateau and isochron age results are nearly the same. The weighted average yields an age of 9.24 ± 0.09 Ma.

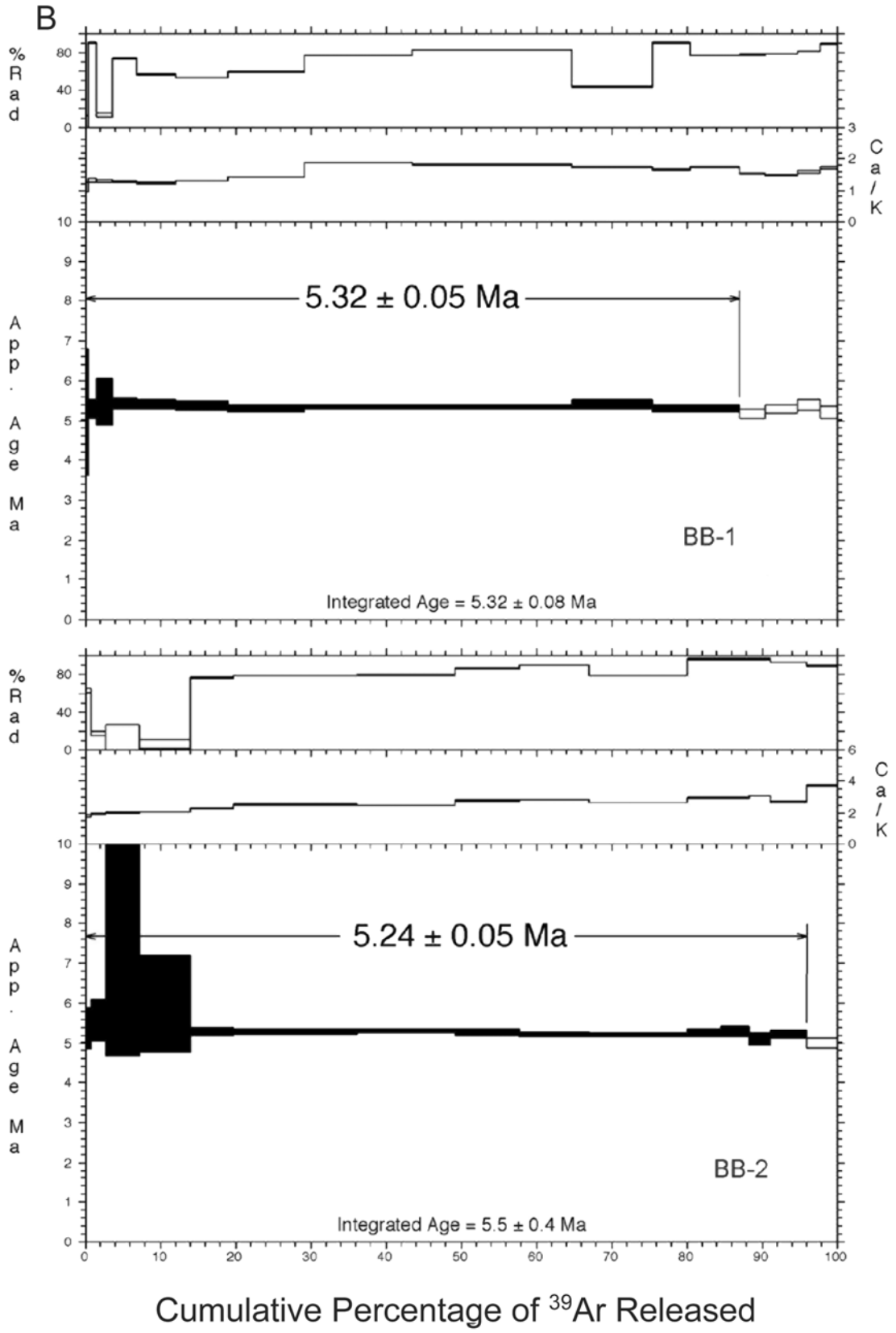

Fig. 16. *Continued.* b) $^{40}Ar/^{39}Ar$ incremental heating spectra for clast-free fractions from two samples (BB-1 at top and BB-2, bottom) from Bahía Blanca, yielding an age of 5.28 ± 0.04 Ma, as discussed in the text.

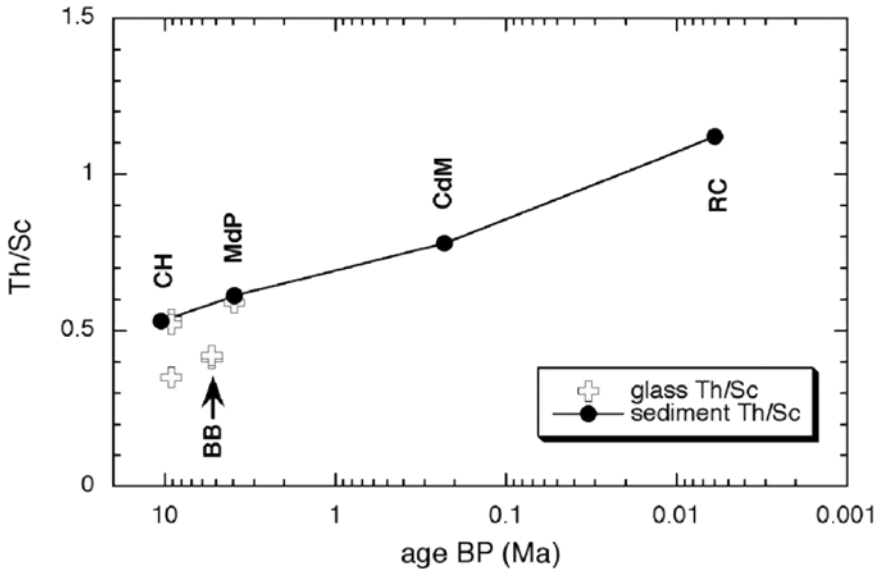

Fig. 17. Changes in Th/Sc values for sediments benchmarked by dated impact glasses from Rio Cuarto (RC), Centinela del Mar (CdM), Mar del Plata (MdP), and Chasicó (CH). The increase in Th/Sc values since the Miocene reflect either evolving source regions through time from basaltic andesitic toward andesitic or incorporation of a more mafic source region at depth. Impact glasses from Chasicó (CH) and Bahía Blanca (BB) suggest even less silicic sources indicating different source materials, perhaps due to incorporation of materials from depth.

Chasicó impact glasses are primarily exposed along portions of a river section that has incised upper Miocene sediments, whereas the 5.2 Ma Bahía Blanca glasses occur in isolated exposures and quarries higher in the stratigraphic section. Obvious primary ejecta facies have not yet been confidently identified, other than concentrations of large impact glass masses. In both cases, the size of the impact glasses and clustered fields suggests a nearby parent crater.

The CH and BB glass compositions from SBA locations generally resemble each other, but differ significantly from the Pliocene and Pleistocene glasses exposed near Mar del Plata. These differences reflect contrasting source materials both in location and depth (time).

Ratios of bulk glass major elements for CH and BB to the host sediments also indicate enrichment in K_2O and P_2O_5 relative to the host sediments, but little difference in other constituents (Fig. 4). Other differences are revealed by unmelted minerals and clasts, normative calculations for certain glasses, quench crystals, and trace elements.

The much greater fraction of unmelted Ca-pyroxenes in the CH and BB glasses indicate a mix of more pristine mafic components than sediments found elsewhere in SBA. The range in bulk compositions of the glasses and the quench crystals also indicate more mafic precursors. Although high barium levels (2000 ppm) could be attributed to entrained mafic lasts, the extremely high level of Ba (~7600 ppm) in CH-1 is not associated with increases in other trace elements (Hf, Eu, Tb), as would be expected if it were from a purely mafic source. Such a large enhancement may represent either excavation of barium-rich evaporates (or hydrothermal deposit) or incorporation of biogenic barite from the water column (if a shallow marine impact). Alternatively, enrichment by post-impact hydrothermal processes could have played a role.

This particular glass may have incorporated Tertiary marine sequences, which are known to occur at depth, or hydrothermal alteration. More detailed analyses will be necessary to understand the significance of such components.

Comparisons of V, Rb, La, Th, Sc, and other minor and trace elements of both the bulk sediments and impact glasses from SBA reveal systematic changes over time (Table 5). The differences can be understood by the increasing contributions from Andean volcaniclastics (and transport by-products) associated with the late Miocene through Pleistocene Cordilleran uplift (Schultz et al. 2004) or evolving source regions in response to climate and dominant wind direction as noted for the late Pleistocene (Smith et al. 2003). Figure 17 shows this trend in the decreasing value of Th/Sc with increasing age. The generally lower values of Th/Sc for some glasses relative to their host sediments suggest incorporation of materials from depth (e.g., CH-1). The BB samples both have Th/Sc levels lower than even the older Chasicó sediments. More systematic studies may reveal trends related to the proximity to the source crater.

Figure 18 is ternary plot comparing for Th/Sc, La/Th, and La/Sc in the late Cenozoic impact glasses and associated sediments. Both the host sediments and impact glasses from various localities become progressively more silicic with time (to the present), which reflects evolving source areas. Three

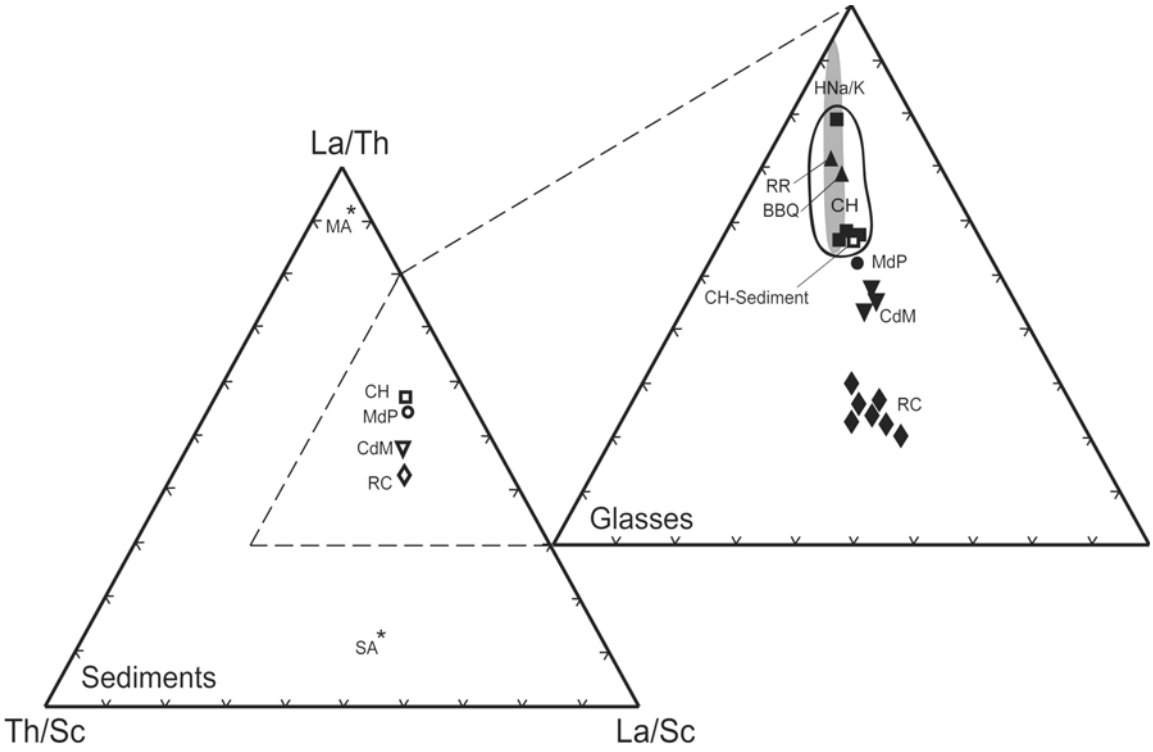

Fig. 18. A ternary diagram illustrating the systematic differences between the compositions of Argentine impact glasses (and the sediments they are found in). RC (Rio Cuarto) represents two events at ~6 ka and ~120 ka. CdM (Centinela del Mar) represents one event at ~445 ka. MdP (Mar del Plata) represents a late Pliocene impact at 3.3 Ma (Schultz et al. 2004). CH (Chasicó) and BB (Bahía Blanca) represent the late Miocene events (~5.3 Ma and ~9.2 Ma, respectively) reported here. Also plotted are the compositions of Holocene mafic ash (MA) deposits (MA) and Pleistocene silicic ash (SA) recovered from the sections. The cutout shows values for glasses (filled symbols) relative to sediments at Chasicó (open square). CH and BB glasses follow the same thread but are generally less silicic than the Miocene host sediments at Chasicó. CH impact glasses are more mafic than the host sediments; consequently, the CH impact may have excavated unexposed units at depth. The shaded field indicates the range of compositions (from Chapman and Scheiber [1969]) for the ~10 Ma (Bottomley and Koeberl 1999) HNa/K tektites.

of the analyzed glasses (one from BB, the others CH) indicate source materials significantly less silicic.

Consequently, the impact glasses of Chasicó generally represent fused surface sediments reworked from volcanic fines and silts from the Miocene. While they generally resemble the composition of other post-Miocene glasses, the Miocene glasses differ by being generally more mafic and having more extensive quench crystallization. Although classified as andesitic (based on major elements), the glasses also contain mafic mineral clasts and a higher fraction of unmelted pyroxenes. Incorporation and decomposition of carbonate-rich claystones or mixed marine deposits also could contribute to locally higher CaO and lower silica contents in the melt in certain samples. The Th/Sc ratios indicate that the BB and some of the CH impacts glasses incorporated less silicic materials (on average) from the Tertiary, prior to the late Miocene uplift responsible for the loessoid sediments comprising most of the Pampas. The greater fraction of unmelted mafic xenocrysts within the CH glasses indicates materials either transported from Miocene mafic volcanics along the eastern Andes or excavated from units not yet sampled at depth.

IMPLICATIONS

Cratering Flux Estimates

The seemingly large number of distinct ages of impact glasses could reflect, at least in part, a northern hemisphere perspective where repeated Pleistocene glaciations eroded, buried, or erased the true impact cratering record. But it also may reflect either an incomplete understanding of atmospheric entry or perhaps even an increased flux rate of interplanetary debris during the late Miocene.

Disparities between predictions for terrestrial crater production rates depend on different approaches and assumptions: above-atmosphere flux rates as a basis for the cratering production rate (e.g., Shoemaker et al. 1990; Chapman and Morrison 1994; Stuart 2001); downward extrapolation of the terrestrial cratering record (e.g., Schultz et al. 2004b [based on Shoemaker et al. 1990]); rates of observed atmospheric bursts (e.g., Brown et al. 2002); and theoretical models of atmospheric disruption and survival (e.g., Bland and Artemeiva 2003; Bland et al. 2004).

Each approach for assessing the likelihood of melt-

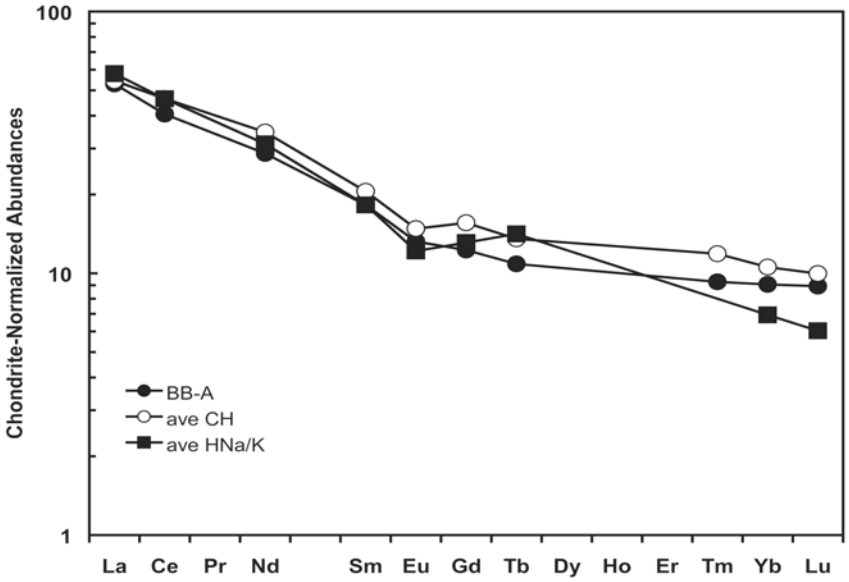

Fig. 19. A comparison of averaged rare earth elements for 9.2 Ma impact glasses from Chasicó (solid squares) and 5.3 Ma glasses from Bahía Blanca (solid circles) with averaged values for tektites with Na/K ratios (from data given by Chapman and Schieber [1969]) shown by open circles. Similarity suggests that Argentine Miocene sediments could represent a viable source region. Radiometric and fission-track ages for the HNa/K glasses also are approximately 10 Ma (Storzer 1985; Bottomley and Koeberl 1999), which is close to the well-constrained radiometric date of the Chasicó glasses.

generating impacts has limitations. The use of either the lunar cratering rates or observations of near-Earth crossing asteroids (NEAs) cannot be simply extrapolated to the surface of the Earth without model assumptions for the survival during atmospheric entry. Estimates of the expected production of craters subject to models of atmospheric disruption (Bland and Artemeiva 2003) yield cratering rates a factor of 100× less than the above-atmosphere rate, 20× less than predictions by Chapman and Morrison (1994), and still about 10× less than extrapolations from large to small craters.

When specifically applied to the cratering rate in all of South America, Bland et al. (2004) estimated that 18 craters > 10 km should have formed during the last 100 Myr. During the last 1 Myr, 1 crater > 1 km, and ~200 Campo del Cielo events should have occurred. More specifically, about 200 small asteroids larger than 50 m across should have encountered the upper atmosphere during the last 10 Myr over an area covered by the Argentine Pampean sediments (~110^6 km) based on rates in Bland and Artemeiva (2003). Their best-fit atmosphere-disruption model predicts, however, that a 50 m object would strike the surface with only a 1-in-5 chance in 10 Myr over 10^6 km^2. Although 100 objects greater than 3–5 m across could have actually impacted over 10 Myr, most (95%) of them would have been irons (possible forming 100 m diameter craters). For comparison, other studies of the observed flux of bolides (atmospheric bursts) from satellite data (e.g., Brown et al. 2002) yield about 20 objects > 50 m in diameter (Tunguska-class), 6 objects > 75 m, and 3 objects > 100 m over an area of 10^6 km^2 in the last 10 Myr.

If the observed production rate of larger craters (> 20 km) is simply extrapolated downwards to smaller craters (1–10 km), then higher cratering rates since the Miocene in Argentina naturally result (e.g., Schultz et al. 2004). For example, more than 900 craters with diameters (D) greater than 10 km should have occurred globally over the last 100 Myr based on the asteroid flux rates (Shoemaker et al. 1990). If the production rate depends on D-2, then the Pampean sediments covering one million square kilometers could contain ~20 craters larger than 1.0 km in diameter over the last 10 Myr, 7 craters over the last 2.5 Myr and perhaps 3 in the last 1.0 Myr. An even larger number of craters would be expected if the dependence has a larger exponent (D-2.5).

It is possible that impact melts (glasses) can be generated from craters as small as 0.5 km in diameter due to soft sediments; for example, Aeouellel, Monturaqui, and Wabar craters all have large quantities of impact glass. This observation, however, still does not address the role of atmospheric disruption, which is believed to prevent the most likely objects (small stony meteoroids) from contributing to the crater population (Bland and Artemeiva 2003).

Consequently, the discovery of at least six occurrences of impact melt preserved in relatively continuous deposits over the last 10 Ma in Argentina may have implications for re-considering models of objects surviving entry to produce craters, a better understanding of melt generation from soft sediments, or additional evidence for an enhanced flux rate over the last 10 Myr. The last suggestion would be consistent with evidence for increased flux of interplanetary dust. Concentrations of ^{3}He relative to ^{4}He are found in ocean floor

sediments between ~3 and 10 Ma (Farley 1995). The unique depositional record of Argentina may be preserving a land record of larger objects during this time as well.

Possible Connection with HNa/K Tektites

Radiometric and fission track ages, 10.2 ± 0.5 Ma (Bottomley and Koeberl 1999) and 8.35 ± 0.90 Ma (1σ) (Storzer 1985) respectively, indicate that the high sodium/potassium (HNa/K) Australian tektites are much older than other Australasian tektites (0.7 Ma) that are found in the same area. However, the age of this enigmatic tektite group is close to the 9.24 ± 0.09 Ma (2σ) age of the Chasicó glasses.

In addition to their age and simple morphologies, HNa/K tektites also are compositionally distinct from members of the Australasian strewn field (Chapman and Schieber 1969; Compston and Chapman 1969; Taylor and Epstein 1969; Montanari and Koeberl 2000) and are believed to have originated from basaltic to andesitic target rocks. Although the CI-normalized REE abundances in HNa/K tektites are significantly lower than in Australasian tektites, their REE patterns (Chapman and Schieber 1969) generally resemble those for CH glasses (Fig. 19).

Ternary plots such as Fig. 18 also are commonly used to differentiate the major tektite strewn fields and their source regions (e.g., Albin et al. 2000). In the comparison of Th/Sc: La/Th: La/Sc, the composition of HNa/K tektites can be explained as a mixture of predominantly mafic basaltic to andesitic rocks with a more Th-rich "continental" component. A nearly identical composition (see Fig. 18) is found in the upper Miocene Pampean sediments (and the CH and BB impact glasses produced from them), which represent mixtures of early Andean volcanics and weathered Patagonian basalts with lesser amounts of eroded basement.

Although further work is necessary to demonstrate the connection, the age of the Chasicó glasses and close similarities in important aspects of both major and trace-element chemistry suggest that a relationship with the HNa/K tektites is plausible. The possibility that Pampas is the source region of HNa/K tektites should be considered. High-velocity molten debris ejected at high angles (e.g., vapor entrained melts) at mid-latitudes result in a preferential re-entry concentration to the west due to the Coriolis force (Wrobel and Schultz 2003), in this case over the Pacific and Australia.

CONCLUDING REMARKS

The Argentine loessoid sequences are yielding an unprecedented archive of well-preserved impact materials dating back to the late Miocene. The 9.24 Ma age Chasicó impact glasses may be associated with a source crater nearby based on the size and distribution of the materials. Although the 5.28 Ma glasses are more widespread due to available exposures, a specific source has not yet been identified. These glasses closely correspond to the Miocene/Pliocene boundary, but a causal relationship cannot yet be inferred. The REE patterns for the Chasicó glasses generally match both the composition and age of the enigmatic HNa/K subgroup of tektites, thereby opening the possibility for a source region quite distinct from the rest of the Australasian strewnfield.

Because the impact glasses establish a precise timeline, they can be used to establish unique chronostratigraphic benchmarks for assessing mammalian evolution, on-land record of paleoclimates, and the evolving source regions. The geochemistry of the bulk sediments reveals previously unrecognized differences related to changes in source regions syngenetic with the late Miocene Andean orogeny. And the differences in compositions between the impact glasses and host sediments provide evidence that the impact incorporated materials from depth, in contrast with Rio Cuarto impact glasses that incorporated near-surface materials (Aldahan et al. 1998; Schultz et al. 2004). Impact glasses also provide critical tracers of processes that result in mixing of associated fossil remains, thereby potentially complicating inferred faunal evolution. The impact glass horizons and reworked materials will contribute to better constrain interpretations of these fossil-rich Miocene sequences (e.g., Zárate et al., Forthcoming) while establishing a new reference for impact products in sedimentary settings.

Editorial Handling—Dr. John Spray

REFERENCES

Albin E. F., Norman M. D., and Roden M. 2000. Major and trace element compositions of georgiaites: Clues to the source of North American tektites. *Meteoritics & Planetary Science* 35:795–206.

Aldahan A. A., Koeberl C., Possnert G., and Schultz P. 1997. ^{10}Be and chemistry of impactites and target materials from the Rio Cuarto crater field, Argentina: Evidence for surficial cratering and melting. *GFF* 119:67–72.

Berggren W. A., Kent D.V., Swisher C.C. III, and Aubry M. P. 1995. A revised Cenozoic geochronology and chronostratigraphy. In *Geochronology, time scales and global stratigraphic correlation*, edited by Berggren W. A. Tulsa, Oklahoma: Society for Sedimentary Geology. pp. 129–212.

Bland P. A., de Souza Filho C. R., Tull A. J. T., Kelley S. P., Hough R. M., Artemieva N. A., Pierazzo E., Coniglio E., Pinotti L., Evers V., and Kearsley A. T. 2002. A possible tektite strewnfield in the Argentine pampas. *Science* 296:1109–1111.

Bland P. A. and Artemieva N. A. 2003. Efficient disruption of small asteroids by Earth's atmosphere. *Nature* 424:288–290.

Bland P. A., Artemieva N. A., and de Souza Filho C. R. 2004. The production rate of small craters on Earth, and the expected crater population in South America (abstract). *Meteoritics & Planetary Science* 39:A16.

Bischoff A. and Stöffler D. 1984. Chemical and structural changes induced by thermal annealing of shocked feldspar inclusions in impact melt rocks from Lappäjarvi crater, Finland. *Journal of Geophysical Research* 89:B645–B656.

Bondesio P., Laza J. H., Scillato Yané G. J., Tonni E. P., and Vucetich M. 1980. Estado actual del conocimiento de los vertebrados de la Formación Arroyo Chasicó (plioceno

temprano) de la provincia de Buenos Aires. *Actas II Congreso Argentino de Paleontología y Bioestratigrafía y I Congreso latinoamericano de Paleontología*. Buenos Aires 1978, T. III, 1980:101–127.

Bonorino A. G., Schillizzi R., and Kostadinoff J. 1987. Investigación geológica y geofísica de la región de Bahía Blanca. *Actas III Jornadas Pampeanas de Ciencias Naturales*. Universidad Nacional de la Pampa, Serie Suplementos 3:55–63.

Brown P., Spalding R. E., ReVelle D. O., Tagliiafieri E., and Worden S. P. 2002. The flux of small Earth-crossing objects colliding with the Earth. *Nature* 420:314–316.

Bottomley R. J. and Koeberl C. 1999. The age of a separate Australasian tektite event. *Meteoritics & Planetary Science* 34: A15.

Bunch T. E. 1968. Some characteristics of selected minerals from craters. In *Shock metamorphism of natural materials*, edited by French B. M. and Short N. M. Baltimore, Maryland: Mono Book Corporation. pp. 413–432.

Carstens H. 1975. Thermal history of impact melt rocks in the Fennoscandian Shield. *Contributions to Mineralogy and Petrology* 50:145–155.

Catti M., Freyria Fava F., Zicovich C., and Dovesi R. 1999. High-pressure decomposition of MCr_2O_4 spinels (M=Mg, Mn, Zn) by ab initio methods. *Physics and Chemistry of Minerals* 26:389–395.

Chapman C. R. and Morrison D. 1994. Impacts on the Earth by asteroids and comets: Assessing the hazard. *Nature* 367:33–40.

Chapman D. R. and Scheiber L. C. 1969. Chemical investigation of Australasian tektites. *Journal of Geophysical Research* 74:6737–6776.

Compston W. and Chapman D. R. 1969. Sr isotope patterns within the Southeast Australasian strewn-field. *Geochimica et Cosmochimica Acta* 33:1023–1036.

Deschamps C. M. 2003. Estratigrafía y paleoambientes en el Cenozoico del sur de la provincia de Buenos Aires. El aporte de los vertebrados. Ph.D. thesis. Facultad de Ciencias Naturales y Museo Universidad Nacional de La Plata, La Plata, Argentina. 317 p.

Devine J. D., Gardner J. L., Brack H. P., Layne G. D., and Rutherford M. J. 1995. Comparison of microanalytical methods for estimating H_2O contents of silicicvolcanic glasses. *American Mineralogist* 80:319–328.

Dressler B. 1990. Shock metamorphic features and their zoning and orientation in the Precambrian rocks of the Manicouagan Structure, Quebec, Canada. *Tectonophysics* 171:229–245.

El Goresy A., Fechtig H., and Ottemann J. 1968. The opaque minerals in impact glasses. In *Shock metamorphism of natural materials*, edited by French B. M. and Short N. M. Baltimore, Maryland: Mono Book Corporation. pp. 531–553.

Farley K. A. 1995. Cenozoic variations in the flux of interplanetary dust recorded by ^{3}He in deep-sea sediment. *Nature* 376:153–156.

Fidalgo F., Laza J. H., Porro N., and Tonni E. P. 1978. Algunas características de la Formación Arroyo Chasicó y sus relaciones geológicas. *VII Congreso Geológico Argentino, Actas I*. pp. 213–225.

French B. M. 1968. Sudbury structure, Ontario: Some petrographic evidence for an origin by meteorite impact. In *Shock metamorphism of natural materials*, edited by French B. M. and Short N. M. Baltimore, Maryland: Mono Book Corporation. pp. 383–412.

French B. M., Cordua W. S., and Plescia J. B. 2004. The Rock Elm meteorite impact structure, Wisconsin: Geology and shock-metamorphic effects in quartz. *Geological Society of America Bulletin* 116:200–218.

Grieve R. A. F., Langenhorst F., and Stöffler D. 1996. Shock metamorphism of quartz in nature and experiment: II. Significance in geoscience. *Meteoritics & Planetary Science* 31: 6–35.

Harris R. S., Schultz P. H., and Bunch T. E. 2005a. Accessory phases in Argentine impact breccias: Implications for shock history, emplacement dynamics, vapor composition and target lithologies (abstract #1952). 36th Lunar and Planetary Science Conference. CD-ROM.

Harris R. S., Schultz P. H., and Bunch T. E. 2005b. Evidence for shocked feldspars and ballen quartz in 450,000 year old Argentine impact melt breccias (abstract #1966). 36th Lunar and Planetary Science Conference. CD-ROM.

Hudon P., Jung I., and Baker D. R. 2002. Melting of β-quartz up to 2.0 GPa and thermodynamic optimization of the silica liquidus up to 6.0 GPa. *Physics of the Earth and Planetary Interiors* 130: 159–174.

Iriondo M. H. 1997. Models of deposition of loess and loessoids in the Upper Quaternary of South America. *Journal of South American Earth Sciences* 10:71–79.

Kieffer S.W. 1971. Shock metamorphism of the Coconino sandstone at Meteor Crater, Arizona. *Journal of Geophysical Research* 76: 5449–5473.

Kieffer S. W., Phakey P. P., and Christie J. M. 1976. Shock processes in porous quartzite: Transmission electron microscope observations and theory. *Contributions to Mineralogy and Petrology* 59:49–93.

Marshall L. G., Hoffstetter R., and Pascual R. 1983. Mammals and stratigraphy: Geochronology of the continental mammal-bearing Tertiary of South America. *Palaeovertebrata*, Montpellier, Mémoir, Extr.: 1–93.

Montanari A. and Koeberl C. 2000. Impact stratigraphy: The Italian record. Berlin:Springer-Verlag. 364 p.

Muhs D. and Zárate M. 2001. Late Quaternary aeolian records of the Americas and their paleoclimatic significance. In *Interhemispheric climate linkages*, edited by Markgraf V. San Diego: Academic Press. pp. 183–216.

Orgeira M. J., Walther A. M., Vasquez C. A., dí Tomasso I., Alonso S., Sherwood G. H., Hu Y. G., and Vilas J. F. A. 1998. Mineral magnetic record of paleoclimatic variation in loess and paleosol from the Buenos Aires formation (Buenos Aires, Argentina). *Journal of South American Earth Sciences* 11:561–570.

Pascual R., Ortiz Jaureguizar E., and Prado J. 1996. Land mammals: Paradigm for Cenozoic South American geobiotic evolution. In *Contributions of southern South America to vertebrate paleontology*, edited by Arratia G. München: Pfeil. pp. 265–319.

Reimold W. U., Kelley S. P., Sherlock S., Henkel H., and Koeberl C. 2004. Laser argon melting of melt breccias from the Siljan impact structure, Sweden—Implications for possible relations to late Devonian extinction events (abstract #1480). 35th Lunar and Planetary Science Conference. CD-ROM.

Renne R. R., Swisher C. C., Deino A. L., Karner D. B., Owens T., and DePaolo D. J. 1998. Intercalibration of standards, absolute ages and uncertainties in ^{40}Ar/^{39}Ar dating. *Chemical Geology* 145: 117–152.

Schultz P. H., Koeberl C., Bunch T. E., Grant J. A., and Collins W. 1994. Ground truth for oblique impact processes: New insight from the Rio Cuarto, Argentina, crater field. *Geology* 22:889–892.

Schultz P., Zárate M., Hames W., Camilión C., and King J. 1998. A 3.3 Ma impact in Argentina and possible consequences. *Science* 282:2061–2063.

Schultz P. H., Zárate M.A., and Hames W. 1999. Three new Argentine impact sites: Implications for Mars (abstract #1898). 30th Lunar and Planetary Science Conference. CD-ROM.

Schultz P. H., Zárate M. A., Hames W., King J., Heil C., Koeberl C., Renne P. R., and Blasi A. 2002a. Argentine impact record. *Abstracts with programs: Geological Society of America*. Boulder, Colorado: Geological Society of America. p. 401.

Schultz P. H., Zárate M. A., King J., Blasi A., Hames W. 2002b. Formation and evolution of impact craters in the Argentine Pampas. *Actas del XV Congreso Geologico Argentino*. pp. 179–181.

Schultz P. H., Zárate M. A., Hames W., Koeberl C., Bunch T. E., Renne P. R., and Wittke J. 2004. The Quaternary impact record from the Pampas, Argentina. *Earth and Planetary Science Letters* 219:221–238.

Sharp W. and Deino A. L. 1996. Laser heating of samples for Ar-Ar geochronology. *Eos* 77:F773.

Shoemaker E. M., Wolfe R. F., and Shoemaker C. S. 1990. Asteroids and comet flux in the neighborhood of Earth. In *Global catastrophes in Earth history: An interdisciplinary conference on impacts, volcanism, and mass mortality*, edited by Sharpton V. L. and Ward P. D. Boulder, Colorado: Geological Society of America. pp. 155–170.

Short N. M. and Gold D. P. 1996. Petrography of shocked rocks from the central peak at the Manson impact structure. In *The Manson impact structure, Iowa: Anatomy of an impact crater*, edited by Koeberl C. and Anderson R. R. pp. 245–265.

Simonson B. M. 2003. Petrographic criteria for recognizing certain types of impact spherules in well-preserved Precambrian successions. *Astrobiology* 3:49–65.

Smith J. V. and Brown W. L. 1988. *Feldspar minerals: Crystal structures, physical, chemical, and microtextural properties*, vol. 1. Berlin: Springer-Verlag. 828 p.

Smith J., Vance D., Kemp R., Archer C., Toms P., King M., and Zárate M. 2003. Isotopic constraints on the source of Argentinian loess-with implications for atmospheric circulation and the provenance of Antarctic dust during recent glacial maxima. *Earth and Planetary Science Letters* 212:181–196.

Stöffler D. 1966. Zones of impact metamorphism in the crystalline rocks at the Nördlinger Ries crater. *Contributions to Mineralogy and Petrology* 12:15–24.

Stöffler D. 1984. Glasses formed by hypervelocity impact. *Journal of Non-Crystalline Solids* 67:465–502.

Stöffler D. and Langenhorst F. 1994. Shock metamorphism of quartz in nature and experiment: Basic observation and theory. *Meteoritics* 29:155–181.

Storzer D. 1985. The fission track age of high sodium/potassium australites revisited. *Meteoritics* 20:765–766.

Stuart J. S. 2001. A near-Earth asteroid population estimate from the LINEAR Survey. *Science* 294:1691–1693.

Taylor H. P. and Epstein S. 1969. Correlations between $^{18}O/^{16}O$ ratios and chemical compositions of tektites. *Journal of Geophysical Research* 74:6834–6844.

Taylor S. R. and McLennan S. M. 1985. *The continental crust: Its composition and evolution*. Oxford: Blackwell. 312 p.

von Engelhardt W. and Stöffler D. 1968. Stages of shock metamorphism in crystalline rocks of the Ries basin, Germany. In *Shock metamorphism of natural materials*, edited by French B. M. and Short N. M. Baltimore, Maryland: Mono Book Corporation. pp. 159–168.

von Engelhardt W. and Bertsch W. 1968. Shock induced planar deformation structures in quartz from the Ries crater. *Contributions to Mineralogy and Petrology* 20:203–234.

White J. C. 1993. Shock-induced amorphous textures in plagioclase, Manicouagan, Quebec, Canada. *Contributions to Mineralogy and Petrology* 113:524–532.

Whitehead J., Spray J. G., and Grieve R. A. F. 2002. The origin of "toasted" quartz in terrestrial impact structures. *Geology* 30:431–434.

Wrobel K. E. and Schultz P. H. Accumulation of distal impact ejecta on Mars since the Hesperian (abstract #3242). Sixth International Conference on Mars. CD-ROM.

Zárate M. 2003. The loess record of Southern South America. *Quaternary Science Reviews* 22:1987–2006.

Zárate M., Schultz P. H., Blasi A., Heil C., King J., and Hames W. Forthcoming. Geology and geochronology of the type Chasicóan (late Miocene) mammal-bearing deposits of Buenos Aires Province (Argentina). *Journal of South American Earth Sciences*.

Zambrano J. 1980. Comarca de la cuenca cretácica del Colorado. *Geología Regional Argentina, volumen II*. pp. 1033–1070.

Zinck J. A. and Sayago J. M. 1999. Loess-paleosol sequence of La Mesada in Tucumán province, northwest Argentina: Characterization and paleo-environmental interpretation. *Journal of South American Earth Sciences* 12:293–310.